THERMODYNAMICS OF LIQUID Fe-C-O ALLOYS

by

OM PRAKASH

DEPARTMENT OF METALLURGICAL ENGINEERING

INDIAN INSTITUTE OF TECHNOLOGY KANPUR

JUNE, 1986

THERMODYNAMICS OF LIQUID Fe-C-O ALLOYS

A Thesis Submitted

in Partial Fulfilment of the Requirements

for the Degree of

MASTER OF TECHNOLOGY

by

OM PRAKASH

to the

DEPARTMENT OF METALLURGICAL ENGINEERING

INDIAN INSTITUTE OF TECHNOLOGY KANPUR

JUNE, 1986

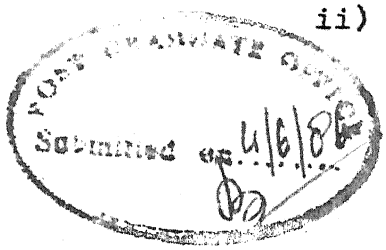

CERTIFICATE

Certified that this work on "Thermodynamics of Liquid Fe-C-O Alloys" has been carried out by Mr.Om Prakash under my supervision and that it has not been submitted elsewhere for a degree.

June, 1986

Brahma Deo

(Dr. Brahma Deo)
Department of Metallurgical Engg.
Indian Institute of Technology
Kanpur-208016

ACKNOWLEDGEMENTS

I wish to express my deep sense of gratitude to Dr. Brahma Deo for his able guidance and constant cooperation right from inception, to the successful completion of this thesis at I.I.T. Kanpur.

I also wish to thank:

- Dr. U.K. Banerjee, Sr. RE, R.D. C.I.S., Ranchi for his important suggestions and for supplying the industrial data related to Chapter 2 of my thesis work.
- Mr.G. Balachandran for his fruitful suggestions at various stages of the work.
- Mr. Sudhir Kumar, Department of Electrical Engineering for his assistance in the computer programming.
- Mr.U.S. Misra for very patiently typing of manuscript.
- Mr.Avadesh Sharma for providing laboratory facilities and helping in initial part of my work.

-Om Prakash

CONTENTS

		Page
	LIST OF TABLES	vi)
	LIST OF FIGURES	viii)
CHAPTER 1	ASSESSMENT OF EQUILIBRIUM CONSTANTS AND INTERACTION PARAMETERS IN LIQUID Fe-C-O ALLOYS	
1.1	Introduction	1
1.2	Scope of Present Work	1
1.3	Review of Previous Work	2
1.4	Theoretical Considerations	5
1.4.1	Method of Evaluation of Interaction Parameters and Equilibrium Constant for the Reaction $\underline{C} + \underline{O} = CO(g)$	6
1.4.2	Method of Evaluation of Interaction Parameters and Equilibrium Constant for Reaction $CO + \underline{O} = CO_2$	14
1.4.3	Method of Evaluation of Interaction Parameters and Equilibrium Constant for Reaction $CO_2 + \underline{C} = 2CO$	14
1.5	Experimental Data Employed	15
1.6	Results and Discussion	15
1.7	Conclusions	27
	REFERENCES	38
CHAPTER 2	EFFICACY OF USE OF OXYGEN PROBES FOR DEOXIDATION STUDIES IN OXYGEN STEEL MAKING	
2.1	Introduction	40
2.2	Scope of Present Work	41
2.3	Oxygen in Molten Steel	42
2.4	Oxygen Sensor-Principle and Application	43
2.5	Practice of Deoxidation of Steel	44
2.6	Thermodynamics of Deoxidation of Steel	46
2.6.1	Thermodynamics of Simple Deoxidation	47
2.6.1.1	Deoxidation with Manganese	50
2.6.1.2	Deoxidation with Silicon	50
2.6.1.3	Deoxidation with Aluminium	51
2.6.2	Thermodynamics of Complex Deoxidation	57

		Page
2.7	Experimental Details	61
2.8	Results and Discussion	62
	2.8.1 Activity Measurements at Turndown	62
	2.8.2 Activity Measurements after Deoxidation	65
2.9	Conclusions	72
	REFERENCES	74
	APPENDIX	
	I Computer Program for Linear Regression	
	II Subroutine for Multiple Linear Regression	
	III Computer Program for Simple Aluminium Deoxidation	
	IV Computer Program for Silicon Manganese Deoxidation	
	V Computer Print out of the Results	

LIST OF TABLES

Table	Title	Page
1.1	Compilation of equilibrium constants for the reaction $\underline{C} + \underline{O} = CO$	3
1.2	Compilation of values of interaction parameters reported by various workers	4
1.3	Experimental data of Noboru Matsumoto at 1500°C at P_{CO} = 16,8 atmospheres	16
1.4	Experimental data of Noboru Matsumoto at 1500°C at P_{CO} = 4,1 atmospheres	17
1.5	Experimental data of El-Khaddah and Robertson for gas mixture CO-1.1 pct CO_2	18
1.6	Experimental data of Banya and Matoba at 1460°C	19
1.7	Experimental data of Banya and Matoba at 1560°C	20
1.8	Experimental data of Banya and Matoba at 1660°C	21
1.9	Experimental data of Banya and Matoba at 1760°C	22
1.10	Parameters used and estimated in different models	29
1.11	Equilibrium constants and interaction parameters obtained from the experimental data of Noboru Matsumoto at 1500°C	30
1.12	Equilibrium constants and interaction parameters obtained from experimental data of El-Khaddah and Robertson for reaction $\underline{C} + \underline{O} = CO$	32

Page

1.13	Equilibrium constants and interaction parameters obtained from experimental data of El-Khaddah and Robertson for reaction $CO + \underline{O} = CO_2$	33
1.14	Equilibrium constants and interaction parameters obtained from experimental data of Banya and Matoba using Model 1	34
1.15	Equilibrium constants and interaction parameters obtained from experimental data of Banya and Matoba using Model 2	35
2.1	Details of oxygen activities and bath analysis at turndown (Data obtained from trials at Rourkela Steel Plant, Rourkela)	67
2.2	Details of oxygen activities and ladle analysis after deoxidation (Data obtained from trials at Rourkela Steel Plant, Rourkela).	68

LIST OF FIGURES

Figure	Title	Page
1.1	Comparison of Log K vs 1/T for the reaction $\underline{C} + \underline{O} = CO$	36
1.2	Comparison of Log K vs 1/T for the reaction $CO + \underline{O} = CO_2$	37
2.1	Schematic diagram of commercial oxygen sensors	45
2.2	Comparison of manganese-oxygen equilibria at 1600°C	54
2.3	Comparison of silicon-oxygen equilibria at 1600°C	55
2.4	Aluminum-oxygen equilibria in steel at 1600°C	56
2.5	Silicon-manganese complex deoxidations activities of residual oxygen and silicon after deoxidation at 1500°C at various activities of residual manganese	60
2.6	Plot of oxygen activity measured by CELOX probes at turndown and predicted oxygen from regression equation	69
2.7	Relation between oxygen activity measured by CELOX probes and oxygen activity determined from thermodynamics of deoxidation reaction ($\underline{Si} + 2\ MnO = SiO_2 + 2\ Mn$)	70
2.8	Relation between oxygen activity measured by RELOX probes and oxygen activity determined from thermodynamics of deoxidation reaction ($2\ \underline{Al} + 3\ \underline{O} = Al_2O_3$)	71

ABSTRACT

Thermodynamics of liquid Fe-C-O alloys forms the basis of thermo-chemical modelling of steel making operations. In the present work a critical review of thermodynamics of Fe-C-O system has been made in Chapter 1. Values of equilibrium constant for reaction $\underline{C} + \underline{O} = CO$ and interaction parameters (e_O^C, e_C^O and e_C^C) reported by several investigators have been compiled. The best set of experimental data reported by various investigators for Fe-C-O liquid system in the temperature range 1500-1760°C have been listed. First and second order interaction parameters (e_O^C, r_O^C) and equilibrium constants have been estimated considering two reactions $\underline{C} + \underline{O} = CO$ and $CO + \underline{O} = CO_2$. Six different computer calculation models were employed. A new value of e_O^C at 1600°C based on Banya and Matoba's experimental data has been recommended. Also, new and more reliable equations of Log K vs $\frac{1}{T}$ have been obtained for both the above reactions.

Recently, oxygen sensors have been employed in industry to directly determine oxygen activity in bath and this in conjunction with thermodynamic data on Fe-C-O systems have been used to predict deoxidation additions. In Chapter 2 principles of oxygen sensor applications in studying deoxidation equilibria have been discussed. Thermodynamics of both simple and complex deoxidation have

been explained. A set of experimental data was obtained from Rourkela Steel Plant, Rourkela. This comprised of (a) bath analysis and temperature at turndown (b) ladle analysis and temperature after deoxidation and (c) oxygen activities measured with oxygen probes. The data were critically analysed in the present work for the first time. Attempt was made to derive a regression equation between oxygen activity measured at turndown by CELOX probes and bath composition and temperature. Also a comparison has been made between oxygen activity measured with CELOX probes after deoxidation in ladle and the thermodynamically calculated oxygen activity from simple (Al) and complex (Si-Mn) deoxidation in order to assess if equilibrium in the bath was attained under industrial conditions.

CHAPTER 1

ASSESSMENT OF EQUILIBRIUM CONSTANTS AND INTERACTION PARAMETERS IN LIQUID Fe-C-O ALLOYS

1.1 Introduction

The thermodynamics of liquid iron containing dissolved carbon (C) and oxygen (O) in equilibrium with $CO-CO_2$ gas mixtures at a given temperature and pressure requires consideration of two of the following three reactions:

$$\underline{C} + \underline{O} = CO\,(g) \qquad (1.1)$$

$$CO\,(g) + \underline{O} = CO_2\,(g) \qquad (1.2)$$

$$CO_2(g) + \underline{C} = 2CO\,(g) \qquad (1.3)$$

If experimental data on equilibrium partial pressures of gases CO_2 and CO and also C and O contents in metal are available the true equilibrium constants (at infinite dilution) as-well-as interaction parameters can be determined. In doing so, one has to assess the accuracy and reproducibility of reported experimental methods and analytical techniques employed.

1.2 Scope of Present Work

A review of literature[1-21] shows that although there is a general agreement in the values of the true equilibrium constants the reported values of interation

parameters differ widely from each other. Table 1.1 gives some equilibrium constant values for reaction (1.1) where as Table 1.2 summarises values of e_C^O, e_C^C, e_O^C and e_O^O reported in various investigations. It may be noted from this table that disagreement is the greatest in the case of e_O^C and e_C^O, where the values differ not only in the magnitude but also in sign. For example, in the recent work reported by Elkhaddah and Robertson[10] and Matsumoto[12], the sign of e_O^C and e_C^O is positive while all others have reported a negative value.

In general, the differences in interaction parameter values have been attributed to experimental and analytical errors and in each subsequent investigations, respective authors credited their own value as being correct. The carbon-oxygen reaction plays an important role in steel refining and therefore a critical evaluation of interaction parameter values and equilibrium constant is necessary. The present work deals specifically with critical evaluation of e_C^O and e_O^C and the equilibrium constants for reactions (1.1) to (1.3) on the basis of data reported in the literature to-date.

1.3 Review of Previous Work

In 1955, Chipman first evaluated the interaction parameters e_C^C and e_C^O/e_O^C based on the then available data of Marshall and Chipman[23]. The scatter in their data was

TABLE 1.1 : Equilibrium Constants for the Reaction

$$\underline{C} + \underline{O} = CO(g)$$

(taken from Reference 22)

Authors	Date of Publi-cation	Equation	Log K_{1600}
1.Chipman and Samarin	1937	$\text{Log } K = \frac{2400}{\text{temp}} + 0.675$	1.956
2.Mccance	1938	$\text{Log } K = \frac{6320}{\text{temp}} - 1.333$	2.041
3.Marshall and Chipman	1942	$\text{Log } K = \frac{1860}{\text{temp}} + 1.642$	2.635
4.Basic OH Steel Making	1944	$\text{Log } K = \frac{2065}{\text{temp}} + 1.643$	2.745
5.Chipman	1955	$\text{Log } K = 2.67 - 0.22(\%C)$	2.626
6.Turkdogan	1955	$\text{Log } K = \frac{1056}{\text{temp}} + 2.131$	2.695
7.Fuwa and Chipman	1960	$\text{Log } K = \frac{1168}{\text{temp}} + 2.07$	2.694
8.Polyakov	1961	$\text{Log } K = \frac{2975}{\text{temp}} + 1.06$	2.649
9.Banya and Matoba	1962	$\text{Log } K = \frac{1160}{\text{temp}} + 2.0$	2.619
10.Elliott	1963	$\text{Log } K = \frac{1169}{\text{temp}} + 2.07$	2.696

TABLE 1.2 : Values of Interaction Parameters reported by various Workers

e_c^c		e_o^c/e_c^o			e_o^o	
Value	Ref.	e_o^c	e_c^o	Ref.	Value	Ref.
0.19	1,2	-0.485	-0.65	11	-.13	16
0.21	3	-0.36	-0.485	4	-.17	11,17
0.22	4-6	-0.34	-0.456	6	-.20	18
0.225	7	-0.421	-0.313	8	-.47	19
0.298	8	-0.45	-0.34	9	-.52	20
0.14	9	+0.05	-	12	0.0	21
0.12	10	+0.1	+.075	10	-.20	9
		-0.28	-	13		
		-0.49	-	14		
		-0.67	-	15		

large. In 1970, Chipman[24] reviewed the thermodynamics of the iron-carbon system and amongst the papers reviewed by him, he considered the works by Rist and Chipman[3], Richardson and Dennis[1] and Banya and Matoba[8] as best. However, Rist and Chipman[3] and Richardson and Dennis[1] studied only CO_2-$\underline{C}$-CO equilibria and did not analyse dissolved oxygen in iron. Banya and Matoba[8] determined e_c^c and e_o^c/e_c^o. In 1974, Sigworth and Elliott[9] tabulated after careful re-evaluation, the interaction parameters in dilute liquid alloys. For Fe-$\underline{C}$-$\underline{O}$ system they too considered the work by Banya and Matoba as best from the point of view of experimental work in relatively dilute solutions.

Fischer and Ackerman[11], Matsumoto[12] and El-Khaddah and Robertson[10] extended their study into higher carbon ranges. Fischer and Ackerman[11] found that e_c^o and e_o^c varied with carbon concentration and their values became less negative with increasing carbon content. Unfortunately, their experimental data are not available. Both Matsumoto[12] and El-Khaddah and Robertson[10] reported positive values of e_o^c and e_c^o.

1.4 Theoretical Considerations

Equilibrium constants for the reactions (1.1) to (1.3) can be written as

$$K_1 = \frac{p_{CO}}{h_c \cdot h_o} \qquad (1.4)$$

$$K_2 = \frac{P_{CO_2}}{P_{CO} \cdot h_O} \qquad (1.5)$$

$$K_3 = \frac{P_{CO}^2}{P_{CO_2} \cdot h_C} \qquad (1.6)$$

where h_O and h_C represent Henrian activity for oxygen and carbon with respect to 1 wt percent as standard state. In the present work both simple and multiple linear regression were employed to determine equilibrium constants and interaction parameters.

1.4.1 Method of Evaluation of Interaction Parameters and Equilibrium Constant for the Reaction $\underline{C} + \underline{O} = CO(g)$

After taking logarithm equation (1.4) can be written as

$$\text{Log } K_1 = \text{Log}[P_{CO}] - \text{Log}[h_C] - \text{Log}[h_O] \qquad (1.7)$$

where

$$h_C = f_C[\text{wt \% C}] \qquad (1.8)$$

$$h_O = f_O[\text{wt \% O}] \qquad (1.9)$$

f_C and f_O are Henrian activity co-efficients. Substituting in equations (1.8) and (1.9) in equation (1.7),

$$\text{Log } K_1 = \text{Log}[P_{CO}] - \text{Log}[\text{wt \%C} \cdot f_C] - \text{Log}[\text{wt \% O} \cdot f_O] \qquad (1.10)$$

or

$$\text{Log } K_1 = \text{Log}[P_{CO}] - \text{Log}[\text{wt\% C}] - \text{Log}[\text{wt\% O}] - \text{Log}[f_C] - \text{Log}[f_O] \qquad (1.11)$$

If 1 wt percent standard state based on Henry's law is adopted then the partial excess Gibbs free energy of mixing $G_i^E = RT \ln f_i$ can be expanded by Taylor's series

$$RT \text{ Log } f_i = RT \text{ Log } f_i^o + \sum_{j=2}^{n} RT \frac{\partial \text{ Log } f_i}{[\partial \text{wt\% } j]} [\text{wt\% } j] + \sum_{j=2}^{n} \frac{1}{2} RT \frac{\partial^2 \text{ Log } f_i}{\partial [\text{wt\% } j]^2} [\text{wt\% } j]^2 + \ldots . \quad (1.12)$$

Higher terms are neglected due to their very small contribution.

Using notations of interaction coefficients equation (1.12) is simplified to

$$\text{Log } f_i = \sum_{j=2}^{n} e_i^j [\text{wt\% } j] + \sum_{j=2}^{n} r_i^j [\text{wt\% } j]^2 \quad (1.13)$$

The activity coefficient f_i^o is assigned the value of 1 at infinite dilution and hence the first term of equation (1.12) has been dropped. e_i^j and r_i^j are respectively the first and second order interaction parameters given by the following equations:

$$e_i^j = \frac{\partial \text{ Log } f_i}{\partial [\text{wt\% } j]} \quad (1.14)$$

$$r_i^j = \frac{\partial^2 \text{ Log } f_i}{[\text{wt\% } j]^2} \quad (1.15)$$

If second order interaction parameter terms are neglected, Log f_i and Log f_o can be written as

$$\text{Log}[f_C] = e_C^C[\text{wt\% C}] + e_C^O[\text{wt\% O}] \quad (1.16)$$

$$\text{Log}[f_O] = e_O^O[\text{wt\% O}] + e_O^C[\text{wt\% C}] \quad (1.17)$$

Equation (1.11) can be written finally as

$$\text{Log } K_1 = \text{Log}[P_{CO}] - \text{Log}[\text{wt\% C}] - e_C^C[\text{wt\% C}] - e_C^O[\text{wt\% O}]$$
$$- e_O^O[\text{wt\% O}] - e_O^C[\text{wt\% C}] - \text{Log}[\text{wt\% O}] \quad (1.18)$$

If the second order interaction parameters are incorporated, equation (1.18) becomes

$$\text{Log } K_1 = \text{Log}[P_{CO}] - \text{Log}[\text{wt\% C}] - e_C^C[\text{wt\% C}] - e_O^O[\text{wt\% O}]$$
$$- e_C^O[\text{wt\% O}] - e_O^C[\text{wt\% C}] - \text{Log}[\text{wt\% O}]$$
$$- r_O^C[\text{wt\% C}]^2 - r_C^C[\text{wt\% C}]^2 \quad (1.19)$$

A relation exists between e_O^C and e_C^O and is given by[9]

$$e_C^O = \frac{M_C}{M_O} e_O^C + \frac{1}{230} \frac{M_O - M_C}{M_O} \quad (1.20)$$

where M signifies the atomic weight. For carbon and oxygen $M_C = 12$ and $M_O = 16$ hence

$$\frac{M_C}{M_O} = 0.75 \text{ and } \frac{M_O - M_C}{M_O} \cdot \frac{1}{230} = \frac{1}{920}$$

e_C^O can therefore be written in terms of e_O^C as

$$e_C^O = .75 \; e_O^C + 1/920 \quad (1.21)$$

Substituting the value of e_C^O from equation (1.21) into

equation (1.18)

$$\text{Log } K_1 = \text{Log}[p_{CO}] - \text{Log}[\text{wt\% C}] - e_C^C[\text{wt\% C}] - e_O^O[\text{wt\% O}] - .75\, e_O^C[\text{wt\% O}] - \frac{1}{920}[\text{wt\% O}] - e_O^C[\text{wt\% C}] - \text{Log}[\text{wt. \% O}] \quad (1.22)$$

If second order interaction parameter is taken into consideration then equation (1.22) becomes

$$\text{Log } K_1 = \text{Log}[p_{CO}] - \text{Log}[\text{wt\% C}] - e_C^C[\text{wt\% C}] - e_O^O[\text{wt\% O}] - .75\, e_O^C[\text{wt\% O}] - \frac{1}{920}[\text{wt\% O}] - e_O^C[\text{wt\% C}] - \text{Log}[\text{wt\% O}] - r_O^C[\text{wt\% C}]^2 - r_C^C[\text{wt\% C}]^2 \quad (1.23)$$

Since experimental data for partial pressures of CO and CO_2, wt percent carbon and wt percent oxygen may be known from literature[8,10,12] equation (1.22) can be written as

$$\text{Log } K_1 + e_O^C[\text{wt\% C}] + .75[\text{wt\% O}] = \text{Log}[p_{CO}] - \text{Log}[\text{wt\% C}] - e_C^C[\text{wt\% C}] - e_O^O[\text{wt\% O}] - [\text{wt\% O}]/920 - \text{Log}[\text{wt\% O}] \quad (1.24)$$

Similarly equation (1.23) can be written as

$$\text{Log } K_1 + e_O^C[\text{wt\% C}] + .75[\text{wt\% O}] + r_O^C[\text{wt\% C}]^2 = \text{Log}[p_{CO}] - \text{Log}[\text{wt\% C}] - e_C^C[\text{wt\% C}] - e_O^O[\text{wt\% O}] - [\text{wt\% O}]/920 - \text{Log}[\text{wt\% O}] - r_C^C[\text{wt\% C}]^2 \quad (1.25)$$

The right hand terms of the equations (1.24) and (1.25) are known say Y_1 and Y_2 respectively and can be equated to the left hand terms, i.e.

$$Y_1 = \text{Log}[p_{CO}] - \text{Log}[\text{wt\% C}] - e_C^C[\text{wt\% C}] - e_O^O[\text{wt\% O}] - [\text{wt\% O}]/920 - \text{Log}[\text{wt\% O}] \quad (1.26)$$

$$Y_2 = \text{Log}[p_{CO}] - \text{Log}[\text{wt\% C}] - e_C^C[\text{wt\% C}] - e_O^O[\text{wt\% O}] - [\text{wt\% O}]/920 - \text{Log}[\text{wt\% O}] - r_C^C[\text{wt\% C}]^2 \quad (1.27)$$

The equations (1.24) and (1.25) can be represented symbolically as

$$Y_1 = a_1x_1 + a_2x_2 \quad (1.28)$$

and

$$Y_2 = a_1x_1 + a_2x_2 + a_3x_3 \quad (1.29)$$

where

$$a_1 = e_O^C \qquad x_1 = [\text{wt\% C}] + .75[\text{wt\% O}]$$

$$a_2 = \text{Log } K_1 \text{ and } \quad x_2 = 1$$

$$a_3 = r_O^C \qquad x_3 = [\text{wt\% C}]^2 \quad (1.30)$$

A computer program based on the principle of multiple linear regression was written to determine e_O^C, r_O^C and Log K. Principle of multiple linear regression is discussed in Appendix II.

Now, the values of e_O^C, r_O^C and Log K_1 are back substituted in equations (1.24) and (1.25), to express these

equations in the form

$$Y_1 = Y_1'$$

and

$$Y_2 = Y_2' \qquad (1.31)$$

A correlation coefficient and standard error of estimate for equations (1.24) and (1.25) are calculated on the basis of linear regression using the formule

$$\text{Correlation coefficient, } R = \frac{N \sum_{i=1}^{N} X_i Y_i - \sum_{i=1}^{N} Y_i \sum_{i=1}^{N} X_i}{\sqrt{N \sum_{i=1}^{N} X_i^2 - \left(\sum_{i=1}^{N} X_i\right)^2}\sqrt{N \sum_{i=1}^{N} Y_i^2 - \left(\sum_{i=1}^{N} Y_i\right)^2}} \qquad (1.32)$$

and standard error of estimate

$$S = \sqrt{\frac{\sum_{i=1}^{N} Y_i^2 - A \sum_{i=1}^{N} Y_i - B \sum_{i=1}^{N} X_i Y_i}{N - 2}} \qquad (1.33)$$

X_i and Y_i are two variables.

A and B are constants.

N = Number of data.

Principle of simple linear regression is discussed in Appendix I. The first and second order interaction parameters and equilibrium constants can be determined using different models.

Model 1

In solving equation (1.22)

(a) Only first order interaction parameters (e_O^C and e_C^C) are employed.

(b) The value of e_O^O and e_C^C have been taken from standard literature[9].

(c) Log K and e_O^C have been determined by computer program using multiple linear regression.

Model 2

In solving equation (1.23)

(a) Both, first and second order interaction parameters (e_O^C, e_C^C, r_O^C and r_C^C) have been used.

(b) The value of e_O^O, e_C^C and r_C^C have been taken from standard literature[9].

(c) Log K, e_O^C and r_O^C have been determined by computer program using multiple linear regression.

Model 3

In solving equation (1.18)

(a) Only first order interaction parameters have been used.

(b) e_C^O and e_O^O have been taken as zero and e_C^C from literature[9].

(c) Log K and e_O^C have been determined.

Model 4

In solving equation (1.19)

(a) Both, first and second order interaction parameters have been used.

(b) Value of e_C^O, $e_O^O = 0$ and e_C^C, r_C^C have been taken from literature[9].

(c) Log K, e_O^C and r_O^C have been determined.

Model 5

In solving equation (1.18)

(a) Only first order interaction parameters have been used.

(b) Values of e_C^O, e_O^O and e_C^C have been taken from literature[9].

(c) Log K and e_O^C have been determined.

Model 6

In solving equation (1.19)

(a) Both, first and second order interaction parameters have been used.

(b) Values of e_O^O, e_C^C, e_C^O and r_C^C have been taken from literature[9].

(c) Log K, e_O^C and r_O^C have been determined.

1.4.2 Method of Evaluation of Interaction Parameters and Equilibrium Constant for the Reaction $CO + \underline{O} = CO_2$

Similar to equations (1.22) and (1.23), the equilibrium constant for the reaction (1.2) can be expressed as

$$\text{Log } K_2 = \text{Log}\left[\frac{p_{CO_2}}{p_{CO}}\right] - \text{Log}[\text{wt\% O}] - e_O^O[\text{wt\% C}] - e_O^C[\text{wt\% C}] \quad (1.34)$$

$$\text{Log } K_2 = \text{Log}\left[\frac{p_{CO_2}}{p_{CO}}\right] - \text{Log}[\text{wt\% O}] - e_O^O[\text{wt\% O}] - e_O^C[\text{wt\% C}] - r_O^C[\text{wt\% C}]^2 \quad (1.35)$$

while using equations (1.34) and (1.35), the same procedure as given in section 1.4.1 is adopted to calculate interaction parameters, equilibrium constants, correlation coefficients and standard error of estimates.

1.4.3 Method of Estimation of Interaction Parameters and Equilibrium Constant for the Reaction $CO_2 + \underline{C} = 2CO$

Similar to equations (1.22) and (1.23), the equilibrium constant for the reaction (1.3) can be expressed as

$$\text{Log } K_3 = \text{Log}[p_{CO}^2/p_{CO_2}] - \text{Log}[\text{wt\% C}] - e_C^C[\text{wt\% C}] - e_C^O[\text{wt\% O}] \quad (1.36)$$

$$\text{Log } K_3 = \text{Log}[p_{CO}^2/p_{CO_2}] - \text{Log}[\text{wt\% C}] - e_C^C[\text{wt\% C}] - e_C^O[\text{wt\% O}] - r_O^C[\text{wt\% C}]^2 - r_C^C[\text{wt\% C}]^2 \quad (1.37)$$

Again the interaction parameters, equilibrium constant and correlation coefficients are calculated using the same procedure as given in section (1.4.1).

1.5 Experimental Data Employed

As discussed before in the present work only the experimental data employed by Noboru Matsumoto[12], El-Khaddah, M.N. and Robertson[10] and Banya and Matoba[8] were used. Tables 1.3 and 1.4 give the details of carbon concentrations and corresponding oxygen concentrations in liquid iron in equilibrium with carbon-monoxide at 16, 8, 4 and 1 atmospheres at 1500°C (12). Table 1.5 shows the carbon and oxygen activities in the molten iron at CO-1.1 pct CO_2 mixture and at temperatures 1550 and 1650°C (10). Tables 1.6, 1.7, 1.8 and 1.9 show the experimental results of Banya and Matoba[8] in which the equilibrium of CO-CO_2 gas mixtures with carbon and oxygen dissolved in liquid iron at temperatures 1460, 1560, 1660 and 1760°C are shown.

1.6 Results and Discussion

The equations based on models 1-6 which were employed to estimate interaction parameters (e_O^C and r_O^C) and equilibrium constants for reactions (1.1) and (1.2) have already been discussed in sections 1.4.1 and 1.4.2. The salient features of the models are briefly summarised

TABLE 1.3 : Experimental Data of Noboru Matsumoto[12] at 1500°C at P_{CO} (16,8 atmospheres)

Data Set 1			Data Set 2	
	P_{CO} = 16 atmosphere		P_{CO} = 8 atmosphere	
Sl.No.	% C	Oxygen (ppm)	% C	Oxygen (ppm)
1.	0.7	231	0.8	146
2.	1.0	193	1.3	117
3.	1.1	140	1.3	68
4.	1.2	95	1.4	66
5.	1.4	77	1.6	81
6.	1.6	75	1.8	47
7.	1.8	79	2.2	15
8.	1.9	62	2.2	29
9.	2.0	61	2.4	22
10.	2.3	38	2.5	26
11.	2.6	38		
12.	2.9	35		
13.	3.1	24		

TABLE 1.4 : Experimental Data of Noboru Matsumoto[12] at 1500°C at p_{CO} (4,1 atmospheres)

Data Set 3			Date Set 4	
p_{CO} = 4 atmosphere			p_{CO} = 1 atmosphere	
Sl.No.	% C	Oxygen (ppm)	% C	Oxygen (ppm)
1.	0.34	168	1.1	11
2.	1.1	73	1.2	14
3.	1.4	38	1.4	9
4.	1.5	27	2.2	15
5.	1.6	26	2.5	4
6.	1.8	20	2.7	7
7.	1.8	20	3.5	6

Table 1.5 : Experimental Data of El-Khaddah and Robertson[10] for Gas Mixture CO-1.1 pct O_2

Sl.No.	Data set	Pressure (atm)	Temp °C	Carbon (wt%)	Oxygen (ppm)
1.	5	69.71	1550	4.10	43
2.		69.71	1550	4.00	62
3.		39.30	1550	3.15	54
4.		39.10	1550	3.14	58
5.		30.00	1550	2.20	77
6.		20.20	1550	2.20	98
1.	6	70.64	1650	3.53	74
2.		70.42	1650	3.52	94
3.		39.07	1650	2.63	100
4.		38.99	1650	2.63	85
5.		40.00	1650	2.66	91
6.		20.20	1650	1.72	140
7.		20.20	1650	1.72	130

TABLE 1.6 : Experimental Data of Banya and Matoba[8] at 1460°C

Data Set 7

Sl.No.	P_{CO}^2/P_{CO_2}	P_{CO_2}/P_{CO}	% C	% O
1.	846	1.18×10^{-3}	1.39	0.00273
2.	846	1.18×10^{-3}	1.41	0.00242
3.	846	1.18×10^{-3}	1.36	0.00262
4.	1100	9.11×10^{-4}	1.69	0.00210
5.	1100	9.11×10^{-4}	1.80	0.00203
6.	2260	4.40×10^{-4}	2.34	0.00178
7.	2260	4.40×10^{-4}	2.35	0.00173
8.	3120	3.23×10^{-4}	2.56	0.00158
9.	3120	3.23×10^{-4}	2.58	0.00152
10.	3120	3.23×10^{-4}	2.58	0.00177

TABLE 1.7 : Experimental Data of Banya and Matoba[8] at 1560°C

Data Set 8

Sl.No.	P_{CO}^2/P_{CO_2}	P_{CO_2}/P_{CO}	% C	% O
1.	46	2.15×10^{-2}	0.107	0.0226
2.	46	2.15×10^{-2}	0.098	0.0238
3.	104	9.54×10^{-3}	0.215	0.0117
4.	104	9.54×10^{-3}	0.215	0.0101
5.	104	9.54×10^{-3}	0.235	0.0113
6.	104	9.54×10^{-3}	0.227	0.0119
7.	104	9.54×10^{-3}	0.214	0.0114
8.	117	8.50×10^{-3}	0.233	0.0113
9.	117	8.50×10^{-3}	0.229	0.0113
10.	209	4.77×10^{-3}	0.369	0.00652
11.	232	4.29×10^{-3}	0.416	0.00697
12.	232	4.29×10^{-3}	0.411	0.00633
13.	232	4.29×10^{-3}	0.433	0.00606
14.	236	4.22×10^{-3}	0.394	0.00636
15.	304	3.18×10^{-3}	0.579	0.00544
16.	378	2.64×10^{-3}	0.612	0.00666
17.	378	2.64×10^{-3}	0.614	0.00632
18.	378	2.64×10^{-3}	0.698	0.00593
19.	468	2.13×10^{-3}	0.678	0.00515
20.	604	1.65×10^{-3}	0.792	0.00737
21.	604	1.65×10^{-3}	0.824	0.00447
22.	604	1.65×10^{-3}	0.826	0.00536
23.	604	1.65×10^{-3}	0.812	0.00378

TABLE 1.8 : Experimental Data of Banya and Matoba[8] ay 1660°C

Data Set 9

Sl. No.	p^2_{CO}/p_{CO_2}	p_{CO_2}/p_{CO}	% C	% O
1.	71	1.40×10^{-2}	0.091	0.0277
2.	71	1.40×10^{-2}	0.086	0.0282
3.	71	1.40×10^{-2}	0.090	0.0278
4.	91	1.09×10^{-2}	0.133	0.0217
5.	91	1.09×10^{-2}	0.121	0.0205
6.	91	1.09×10^{-2}	0.120	0.0206
7.	162	6.14×10^{-3}	0.185	0.0129
8.	168	5.94×10^{-3}	0.210	0.0120
9.	240	4.15×10^{-3}	0.252	0.0110
10.	468	2.13×10^{-3}	0.495	0.00656
11.	468	2.13×10^{-3}	0.499	0.00673
12.	846	1.18×10^{-3}	0.677	0.00435
13.	1100	9.11×10^{-4}	0.881	0.00397
14.	1100	9.11×10^{-4}	0.842	0.00372
15.	2260	4.40×10^{-4}	1.37	0.00355
16.	2260	4.40×10^{-4}	1.37	0.00268
17.	3120	3.23×10^{-4}	1.59	0.00241
18.	3120	3.23×10^{-4}	1.56	0.00262

TABLE 1.9 : Experimental Data of Banya and Matoba[8] at 1760°C

Data Set 10

Sl. No.	p^2_{CO}/p_{CO_2}	p_{CO_2}/p_{CO}	% C	% O
1.	91	1.09×10^{-2}	0.097	0.0320
2.	117	8.50×10^{-3}	0.105	0.0290
3.	117	8.50×10^{-3}	0.105	0.0290
4.	117	8.50×10^{-3}	0.108	0.0286
5.	232	4.29×10^{-3}	0.185	0.0156
6.	240	4.15×10^{-3}	0.160	0.0171
7.	240	4.15×10^{-3}	0.171	0.0183
8.	468	2.13×10^{-3}	0.386	0.0083
9.	468	2.13×10^{-3}	0.332	0.00859
10.	846	1.18×10^{-3}	0.427	0.00579
11.	1100	9.11×10^{-4}	0.611	0.00507
12.	1100	9.11×10^{-4}	0.603	0.00516
13.	2260	4.40×10^{-4}	0.872	0.00401
14.	2260	4.40×10^{-4}	1.11	0.00362
15.	3120	3.23×10^{-4}	1.27	0.00324
16.	3120	3.23×10^{-4}	1.26	0.00338

in Table 1.10. The results of regression analysis based on these models for the experimental data (Tables 1.6 to 1.9) of Banya and Matoba[8], El-Khoddah and Robertson[10] (Table 1.5) and of Noboru Matsumoto[12] (Tables 1.3 to 1.4) are presented in Tables 1.11 to 1.15.

It may be noted that Murty[25] also used a similar method for thermodynamic analysis of Fe-Al-O, Fe-Cr-O, Fe-V-O and Fe-Zr-O systems. In particular, the Models 3 to 6 in the present work were constructed on the same basis as suggested by Murty. The draw back of Models 3-6 is that while determining e_O^C either the e_C^O value is taken from literature or it is omitted during regression analysis. Mathematically speaking this is not justifiable because there exists a relationship between e_C^O and e_O^C as given by equation (1.20). Therefore it is neither necessary to assume a value of e_C^O nor neglect it and e_C^O should not appear as a parameter in the regression equations. This aspect was correctly accounted for in the improved Models 1 and 2 developed in the present work. Although all the Models 1-6 have been tested for significance of regression coefficients and the best fit estimates of e_O^C, r_O^C and equilibrium constants, the final evaluation should be based on only Models 1 and 2.

Results of the analysis of experimental data of Noboru Matsumoto[10] as presented in Table 1.11 for the reaction

$\underline{C} + \underline{O} = CO$ at single temperature 1500°C show that both for Model 1 (without the effect of second order interaction coefficient r_o^C) and for Model 2 (with r_o^C incorporated) the standard deviations in predicted values of e_o^C and r_o^C (the values in parenthesis) are very high. Incorporation of r_o^C in Model 2 does not improve the estimates compared to Model 1. The equilibrium constant (Log K) values are nearly constant (approximately 2.9) but since the multiple correlation coefficient values in the last column are very low (less than 0.8) even the Log K values are not acceptable. Results of Models 3-6 also show a large variation. Therefore the positive e_o^C (.05) value reported by Noboru Matsumoto may not be considered as correct due to large scatter in their data.

El-Khaddah and Robertson[10] did large number of experiments and analysis of their results at 1550 and 1650°C are presented in Table 1.12 for the reaction $\underline{C} + \underline{O} = CO$ and in Table 1.13 for the reaction $CO + \underline{O} = CO_2$ for specific sets of experimental data given in Table 1.5. There were very few experimental data points at 1750°C and they could not be considered due to large scatter. It is evident from the Table 1.12 that standard deviation in e_o^C values in Model 1 is large. The inclusion of r_o^C in Model 2 does not improve the respective standard deviations in e_o^C and r_o^C. Also the multiple correlation coefficients given in the

last column are generally low. The same is true about e_O^C and r_O^C values determined for the reaction $CO + \underline{O} = CO_2$ in Table 1.13. Multiple correlation coefficients given in the last column in this table are high but since standard deviations in e_O^C and r_O^C are large one is forced to neglect the positive value (0.1) of e_O^C reported by El-Khaddah and Robertson[10].

Banya and Matoba[8] did exhaustive experiments (at 1460, 1560, 1660 and 1760°C) and Table 1.14 gives the results of Model 1 for both the reactions $\underline{C} + \underline{O} = CO$ and $CO + \underline{O} = CO_2$. It may be observed that e_O^C values determined from $\underline{C} + \underline{O} = CO$ have a lower standard deviations than determined from $CO + \underline{O} = CO_2$. The multiple correlation coefficients are high for both the reactions with the incorporation of second order interaction coefficient (Model 2) the results given in Table 1.15 show that standard deviation in e_O^C increases for both the reactions inspite of the fact that there is little effect on multiple correlation coefficient (compared to Model 1 in Table 1.14). Model 1 values in Table 1.14 may therefore be taken as more representative for dilute carbon alloys (where effect of r_O^C is negligible).

One may note the discrepancy in Log K values (in Model 1, Table 1.14) for reaction $\underline{C} + \underline{O} = CO$ at 1460°C which is lower than the value at 1560°C. Interaction parameter

value at 1460 is also high. Obviously, it is advisable to neglect the values of e_o^C and equilibrium constants at 1460°C for both the reactions $\underline{C} + \underline{O} = CO$ and $CO + \underline{O} = CO_2$. Further, e_o^C value at 1560°C (in Table 1.14) is quite low (-.52) whereas at 1660 and 1760°C it attains a near constant value (-.3). This suggests that e_o^C is temperature independent only at higher temperatures. Since, as discussed earlier, standard deviation in e_o^C values is smaller for $\underline{C} + \underline{O} = CO$ than for $CO + \underline{O} = CO_2$ (Model 1 Table 1.14) one may adopt the e_o^C value determined from $\underline{C} + \underline{O} = CO$ (i.e. approximately -0.3) at 1600°C and above. Sigworth and Elliott[9] estimated the e_o^C value from the analysis of Banya-Matoba's data as -.45. It is not known which of the two reactions ($\underline{C} + \underline{O} = CO$ or $CO + \underline{O} = CO_2$) was considered for final evaluation. It is better to consider $\underline{C} + \underline{O} = CO$ reaction than $CO + \underline{O} = CO_2$ because the latter involves experimental measurement of small concentrations of CO_2 and in doing so large error may creep in. At high temperatures equilibrium gases contain predominantly CO (more than 90%) in Fe-C-O equilibria and small analysis errors in CO will not much affect the percent error.

The standard deviations in equilibrium constant values at 1560, 1660 and 1760°C in Table 1.14 for reaction $\underline{C} + \underline{O} = CO$ and $CO + \underline{O} = CO_2$ are very small and using these values one may evaluate by regression analysis

$$\text{Log } K_1 = \frac{2423.26}{T} + 1.367 \qquad (1.38)$$

for $\underline{C} + \underline{O} = CO$ and

$$\text{Log } K_2 = \frac{10415.23}{T} - 5.623 \qquad (1.39)$$

for $CO + \underline{O} = CO_2$.

The values of Log K_1 and Log K_2 against $\frac{1}{T}$ are plotted in Figures 1.1 and 1.2 and show close agreement with those of Banya and Matoba[8] and Marshall and Chipman[23].

For the purpose of thermodynamic calculations however equation 1.38 and equation 1.39 should be taken as better estimates of equilibrium constants because of the rigorous nature of Model 1 employed in present work for analysis of experimental data.

1.7 Conclusions

(1) The regression analysis of experimental data based on Models 1 and 2 for Fe-C-O system reported by Matsumoto[10] and El-Khaddah and Robertson[12] have shown large scatter . Banya and Matoba's data[8] have been analysed for evaluation of interaction parameters and equilibrium constants.

(2) Incorporation of second order parameters r_C^C and r_O^C do not decrease the error in estimates.

(3) Equation (1.1), i.e. $\underline{C} + \underline{O} = CO$ is considered

1600°C and above.

(4) The relationship between Log K and $\frac{1}{T}$ was established for reaction $\underline{C} + \underline{O} = CO$ as

$$\text{Log } K_1 = \frac{2423.26}{T} + 1.367$$

and for the reaction

$$CO + \underline{O} = CO_2 \text{ as Log } K_2 = \frac{10415.23}{T} - 5.623$$

in the range 1560-1760°C. This is in close agreement with results of Banya and Matoba[8] and Marshall and Chipman[23] but should be used in preference to their equations in the temperature range 1560-1760°C.

TABLE 1.10 : Parameters used and Estimated in Different Models

Model	Parameters						
	e_a^o	e_C^C	r_C^C	e_C^o	e_o^C	r_o^C	Log K
1	literature	literature	zero	calculated	estimated	zero	estimated
2	literature	literature	literature	calculated	estimated	estimated	estimated
3	zero	literature	zero	zero	estimated	zero	estimated
4	zero	literature	literature	zero	estimated	estimated	estimated
5	literature	literature	zero	literature	estimated	zero	estimated
6	literature	literature	literature	literature	estimated	estimated	estimated

TABLE 1.11 : Equilibrium Constants and Interaction Parameters obtained from the Experimental Data of Matsumoto[10] at 1500°C

Model employed	CO (atm)	e_O^C	r_O^C	Log K	SEE	MCC	Data set
1.	16	-.018 (.026)	-	2.908 (.057)	.0668	.20	1
	8	.1245 (.082)	-	2.540 (.151)	.138	.471	2
	4	-.003 (.0816)	-	2.725 (.118)	.101	.017	3
	1	-.21 (.0819)	-	2.92 (.183)	.179	.753	4
2.	16	.0054 (.156)	-.0059 (.0398)	2.89 (.138)	.07	.20	1
	8	-.22 (.621)	.099 (.178)	2.81 (.507)	.135	.585	2
	4	-.575 (.357)	.263 (.1616)	2.96 (.175)	.078	.63	3
	1	-.331 (.575)	.027 (.128)	3.04 (.575)	.178	.756	4
3.	16	-.016	-	2.904	-	-	
	8	.126	-	2.53	-	-	
	4	-.001	-	2.72	-	-	
	1	-.209	-	2.927	-	-	

CONTINUED....

TABLE 1.11 (Continued):

Model employed	p_{CO} (atm)	e_o^C	r_o^C	Log K	SEE	MCC	Data set
4.	16	.015	-.008	2.88	-	-	
	8	-.195	.093	2.78	-	-	
	4	-.559	.259	2.94	-	-	
	1	-.327	.0269	3.04	-	-	
5.	16	-.0198	-	2.92	-	-	
	8	.122	-	2.54	-	-	
	4	-.0066	-	2.73	-	-	
	1	-.21	-	2.93	-	-	
6.	16	.0004	-.005	2.89	-	-	
	8	-.205	.095	2.78	-	-	
	4	-.57	.26	2.95	-	-	
	1	-.329	.027	3.04	-	-	

SEE = Standard error of estimate (given in parentheses)

MCC = Multiple correlation coefficient.

TABLE 1.12 : Equilibrium Constants and Interaction Parameters obtained from the Experimental Data of El-Khaddah and Robertson[12] for Reaction $\underline{C} + \underline{O} = CO$

Model employed	Temp (°C)	e_O^C	r_O^C	Log K	SEE	MCC	Data set
1.	1550	.085 (.058)	-	2.62 (.189)	.108	.585	5
	1650	.104 (.0268)	-	2.54 (.073)	.048	.865	6
2.	1550	.191 (.794)	-.0169 (.126)	2.46 (1.1)	.108	.588	5
	1660	.39 (.277)	-.06 (.043)	2.19 (.256)	.042	.899	6

SEE = Standard error of estimate. (given in parenthese)

MCC = Multiple correlation coefficient.

TABLE 1.13 : Equilibrium Constants and Interaction Parameters obtained from the Experimental Data of El-Khaddah and Robertson[12] for Reaction $CO + \underline{O} = CO_2$

Model employed	Temp (°C)	e_O^C	r_O^C	Log K	SEE	MCC	Data set
1.	1550	.125 (.0419)	-	-.147 (.135)	.078	.829	5
	1650	.116 (.029)	-	-.26 (.089)	.054	.86	6
2.	1550	.58 (.498)	-.073 (.079)	-.815 (.743)	.069	.869	5
	1650	.50 (.226)	-.073 (.043)	-.73 (.283)	.045	.92	6

SEE = Standard error estimate (given in parenthese).

MCC = Multiple correlation coefficient.

TABLE 1.14 : Equilibrium Constants and Interaction Parameters obtained from the Experimental Data of Banya and Matoba[8] using Model 1

Type of reaction	Temp (°C)	e_o^C	Log K	SEE	MCC	Data set
1. $\underline{C}+\underline{O}=CO$	1460	-.20 (.0145)	2.53 (.0301)	.0229	.979	7
	1560	-.527 (.0523)	2.69 (.0266)	.059	.910	8
	1660	-.295 (.0174)	2.62 (.0139)	.039	.973	9
	1760	-.273 (.0223)	2.56 (.0143)	.036	.956	10
2. $CO+\underline{O}=CO_2$	1460	-.313 (.0305)	0.1247 (.063)	.048	.96	7
	1560	-.659 (.0543)	0.068 (.02)	.063	.935	8
	1660	-.42 (.0159)	-.254 (.0127)	.036	.988	9
	1760	-.42 (.0292)	-.49 (.0186)	.048	.967	10

SEE = Standard error of estimate (given in parenthese).

MCC = Multiple correlation coefficient.

TABLE 1.15 : Equilibrium Constants and Interaction Parameters obtained from the Experimental Data of Banya and Matoba[8] using Model 2

Type of reaction	Temp (°C)	e_o^C	r_o^C	Log K	SEE	MCC	Data set
1. $\underline{C}+\underline{O}=CO$	1460	-.065 (.233)	-.417 (.0587)	2.408 (.218)	.0225	.98	7
	1560	-.346 (.288)	-.187 (.293)	2.665 (.0596)	.0588	.912	8
	1660	-.390 (.074)	.059 (.0465)	2.630 (.0203)	.0383	.975	9
	1760	-.037 (.082)	-.176 (.059)	2.52 (.0193)	.029	.974	10
2. $CO+\underline{O}=CO_2$	1460	.770 (.286)	-.27 (.072)	-.879 (.269)	.0294	.98	
	1560	-.358 (.283)	-.315 (.291)	.015 (.056)	.062	.94	
	1660	-.53 (.065)	.069 (.0465)	-.233 (.017)	.034	.99	
	1760	-.52 (.130)	.077 (.096)	-.47 (.0294)	.048	.97	

SEE = Standard error of estimate (given in parenthese).

MCC = Multiple correlation coefficient.

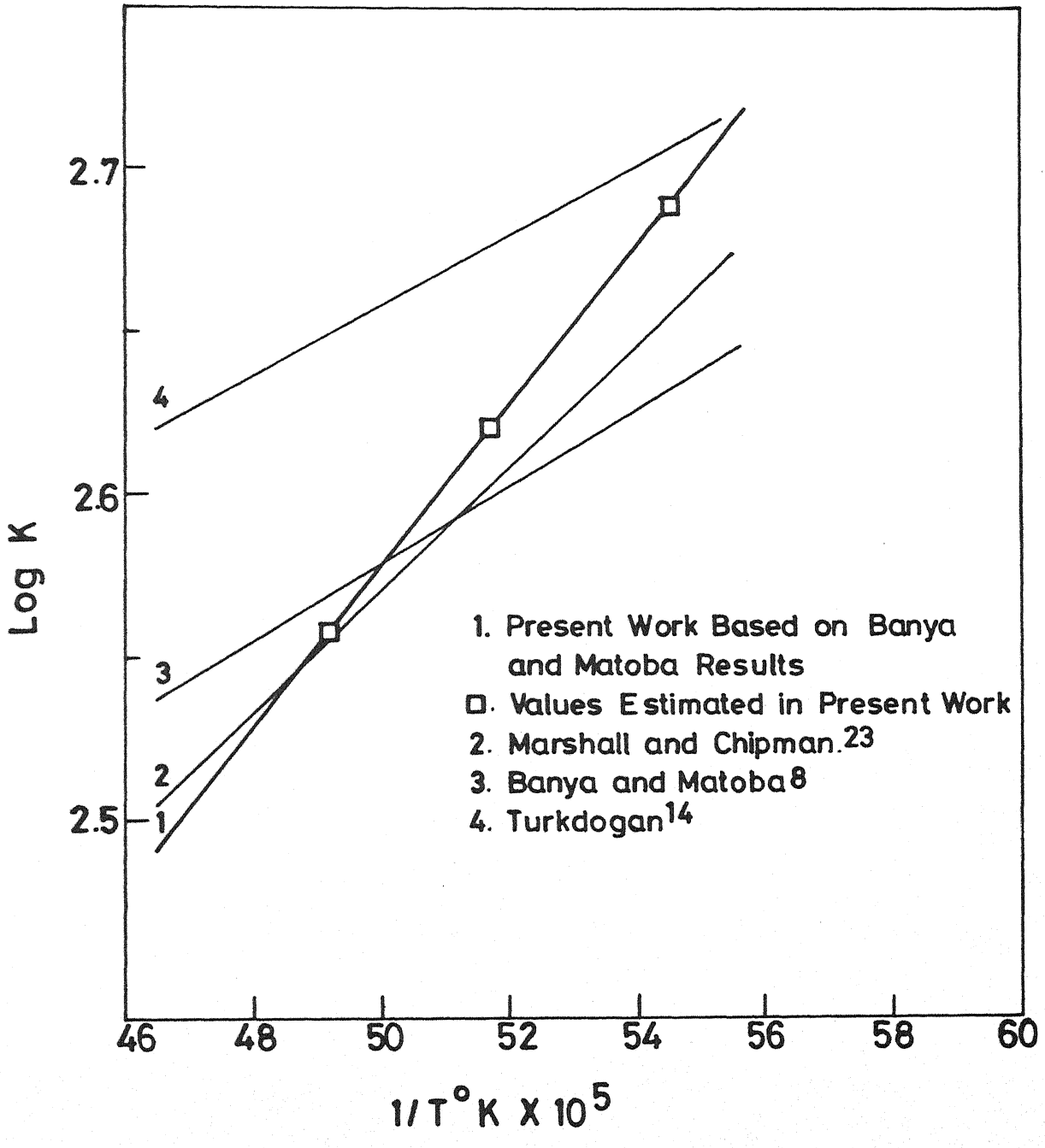

Fig. 1.1 Comparison of Log K Vs 1/T for the Reaction $\underline{C} + \underline{O} = CO$.

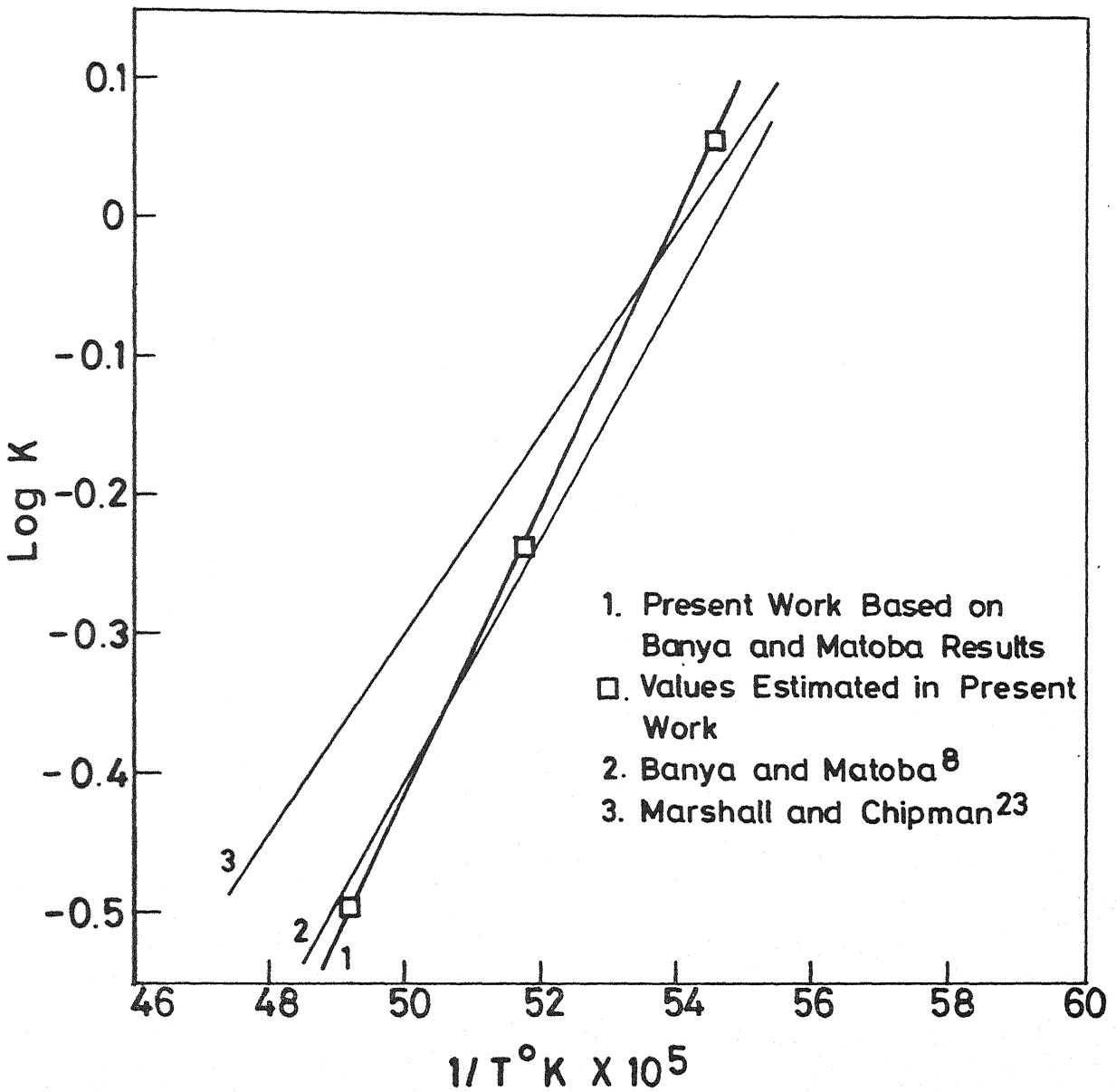

Fig. 1.2 Comparison of Log K Vs 1/T for the Reaction $CO + \underline{O} = CO_2$.

REFERENCES

1. Richardson, F.D. and Dennis, W.E., Trans. Faraday Soc., 1953, Vol. 49, p-171.

2. Shenck, H., and Frohberg, M.G., Arch. Eisenhuttenw, 1962, Vol. 23, p-171.

3. Rist, A. and Chipman, J. Rev. Met., 1957, Vol. 53, p-796.

4. Turkdogan, E.T., Leake, C.E. and Manon, C.R., Acta. Met. 1956, Vol. 4, p-396.

5. Hadrys, H.G., J. Metals., 1968, Vol. 20, p-167.

6. Shenck, H. and Hinze, H., Arch. Eisenhuttenw, 1966, Vol. 37, p-545.

7. Nyquest, O., Lange, K.W. and Chipman, J., 1962, Vol.224, p-714.

8. Banya, S. and Matoba, S., Tetsu to Hagane, 1962, Vol. 48, p-925.

9. Sigworth , G.K. and Elliott, J.F., Metal Science, 1974, Vol. 8, p-298.

10. El-Khaddah, M.N. and Robertson, D.G.C., Met. Trans. B, 1977, Vol.88 , p-569.

11. Fischer, W.A. and Ackerman, W., Arch. Eisenhuttenw, 1965, Vol. 36, 695, 1966, Vol. 27, p-779.

12. Matsumoto, N., Science Reports, Tohoku Univ., 1970, Vol. 22, p-74.

13. Luzgin, V.P., Viskarev, A.F. and Javoiskij, Izvestija Vyssich ucebnych Zavedenij, cernaja Metallurgia 5 (1963), p-442.

14. Turkdogan, E.T., Davis, L.S., Leake, L.E. and Stevens, C.G., J. Iron and Steel Inst., 1955, Vol. 181, p-123.

15. Bennett, G.H.J., Protheroe, H.T. and Ward, R.G., J. Iron and Steel Inst., 1960, Vol. 195, p-174.

16. Shenck, H. and Steinmetz, E., Arch. Eisenhuttenw, 1967, Vol. 38, p-813, p-871.

17. Suwamura, H. and Sano, K., Sub. Comm. for Phys. Chem. of Steel Making, 19th Comm., 3rd Div., Jap. Soc. for Promotion of Science, March 10, 1966.

18. Floridis, T.P. and Chipman, J., Trans. AIME, 1958, Vol.212, p-549.

19. Matoba, S. and Kuwana, T., Testu to Hajane, 1965, Vol. 51, p-163.

20. Gunji, S. and Matoba, S., ibid., 1963, Vol. 49, p-758.

21. Tankins, E.S., Gokcen, U.A. and Belton, G.R., Trans. AIME, 1966, Vol. 220, p-820.

22. Samarin, A.M., Proceedings of Inter. Conf. at Balatonfured, Hungary, 23-26 June, 1970 by ISI, London, p-17.

23. Marshall, S., and Chipman, J., Trans. ASM, 1942, Vol.30.

24. Chipman, J., Met. Trans., 1970, Vol. 1, p-2163.

25. Murty, G.V.R., M. Tech. Thesis, "Thermodynamics of Deoxidation of Molten Iron by Al, Zr, Cr, Ti and V", 1984, p-16.

CHAPTER 2

EFFICACY OF USE OF OXYGEN PROBES FOR DEOXIDATION STUDIES IN OXYGEN STEEL MAKING

2.1 Introduction

It is important to determine and control by proper deoxidation practice the amount of dissolved oxygen in liquid steel before casting because it decides the cleaniness of the steel as well as solidifcation structure (rimmed, killed or semi-killed) of the products made. Until recently, no method was available which could provide the steel maker with a true estimate of dissolved oxygen in the molten steel. Conventional methods (eg. vacuum fusion, inert gas fusion, LECO analysis etc) essentially analysed total oxygen in steel, i.e. dissolved oxygen plus oxygen tied up with the oxide inclusions. Quantity of deoxidisers required to meet the final specification was therefore mainly based on indirect assessment of the dissolved oxygen content of the bath through various means, viz. carbon content of metal, FeO content of the slag and temperature. Since these parameters vary largely from heat to heat, the deoxidation practices were only approximate and not based on scientific judgements.

The development of commercial oxygen probes systems to measure rapidly (in about 25 seconds) and directly "in-situ"

the dissolved oxygen activity in liquid steel aroused great interest through out the steel industry in the hope that the oxygen sensor measurements might provide a basis to formulate scientific procedures to achieve better deoxidation control. In view of this, industrial trials have been conducted at Rourkee Steel Plant, Rourkela by Research and Development Centre for Iron and Steel, Ranchi in the oxygen steel making shop and these have yielded information on suitability of oxygen probes for use in plants.

2.2 Scope of Present Work

In present work, the efficacy of use of commercial oxygen probes to determine oxygen activity in liquid steel has been evaluated based on the results obtained in industrial trials at Rourkela Steel Plant, Rourkela. The oxygen activity in the metal bath can also be thermodynamically calculated from equilibrium constants and interaction parameters. Various deoxidation procedures have been explained and computer programs have been written to evaluate oxygen activity in bath theoretically and then compare it with the measured value obtained through oxygen sensors. This would help to assess whether equilibrium was attained in the bath and therefore the measured value could in any way be used for deoxidation control under

plant conditions.

2.3 Oxygen in Molten Steel

The oxygen content of the liquid steel depends upon temperature and the other alloying elements present such as carbon, silicon, manganese, phosphorus etc. A refined steel may contain 0.01-0.10 wt percent oxygen depending upon its composition. The state in which oxygen is present in liquid iron is still not certain. The existance of FeO molecules or oxides like Fe_2O, Fe_3O or Fe_zO in liquid seems improbable. The dissolution reaction of oxygen in liquid iron can be written as

$$\frac{1}{2}\ O_2\ (g) = \underline{O} \qquad (2.1)$$

where $\underline{O}$ denotes dissolved oxygen in metal.

The Henrian activity of oxygen 'h_o' (with reference to 1 wt percent solution as standard state) at T°K in liquid iron is given as[1]

$$\text{Log } h_o = -\frac{6372}{T} + 2.73 \qquad (2.2)$$

where

$$h_o = (\%\ O) \cdot f_o \qquad (2.3)$$

The activity coefficient f_o in Fe-O system is given as[2]

$$\text{Log } f_o = -0.2 \cdot (\%\ O) \qquad (2.4)$$

The content of dissolved oxygen can be obtained with the help

of oxygen activity coefficient and oxygen activity determined by oxygen sensors using equation (2.3). For alloy steels, the effect of various alloying elements on activity coefficients, f_o is written as[3]

$$\text{Log } f_o = e_o^o \cdot \text{wt\% O} + e_o^x \cdot \text{wt \% x} \qquad (2.5)$$

where e_o^x (X = C, Si, Mn,....) is the first order interaction parameter.

2.4 Oxygen Sensor Principle and Application

The measurement of oxygen activity using oxygen sensor is based on the use of solid electrolytes (solid-solution of oxides of ZrO_2 + 10% CaO) which is capable of conducting electricity by the transport of oxygen anions. When two different oxygen partial pressures are applied across such an electrolyte the system constitutes an oxygen concentration cell expressed by equation

$$\text{Pt, } pO_2^I/\text{Solid electrolyte}/pO_2^{II}\text{, Pt} \qquad (2.6)$$

and the emf developed is governed by Nernst equation[4]

$$E = \frac{RT}{nF} \ln pO_2^{II}/pO_2^I \qquad (2.7)$$

where E = emf across a solid electrolyte (volts)

R = gas constant (J/mole/°K)

F = Faraday constant (J/V/gm equivalent)

T = absolute temperature (°K)

pO_2^I = oxygen partial pressure at the reference electrode

pO_2^{II} = oxygen partial pressure in liquid steel

n = number of electrons (charges) involved in the cell reaction.

A gas with known pO_2 can serve as reference electrode e.g. air is blown into a Pt-solid electrolyte interface. Alternatively, a mixture of a metal and its oxide powder for example $Cr-Cr_2O_3$ and $Mo-Mo\ O_2$ may be used.

After about two minutes of the end of blow the oxygen probes are immersed into the steel bath below slag surface (to a depth greater than 300 mm). The emf rises to a peak value in 4.5 seconds after immersion of probe, stays constant for about 10 seconds and then gradually decreases. The emf (in millivolts) and temperature (°C) are recorded simultaneously. Some typical probe designs[5] are shown in Figure 2.1.

2.5 Practice of Deoxidation of Steel

Deoxidation can be carried out in furnace, ladle or in mold itself by adding suitable deoxidisers. Choice of deoxidation method depends upon the type of steel. Rimmed steel is usually tapped without addition of deoxidisers to the steel in the furnace and only a small addition is made to steel in the ladle. During solidification, there

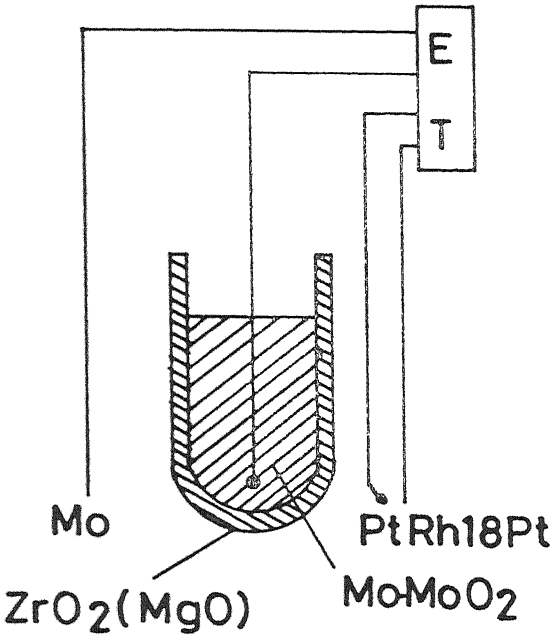

(a) Oxytip Sensor

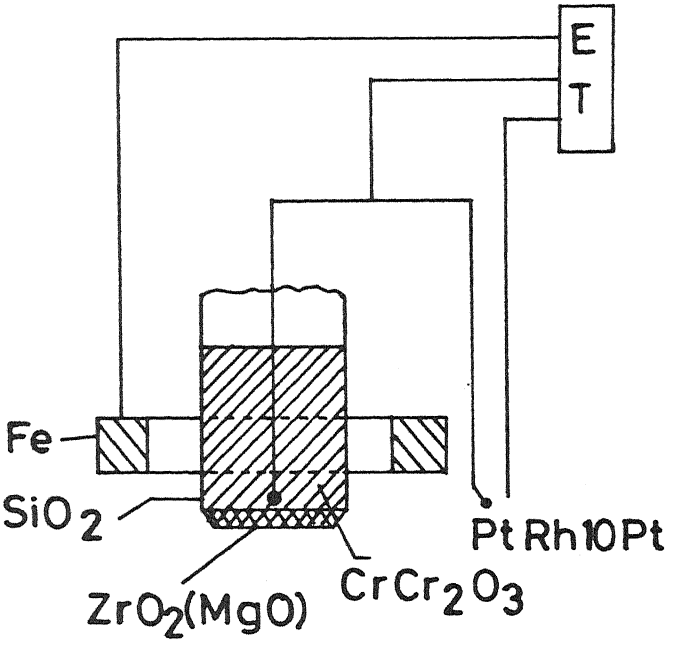

(b) Celox Sensor

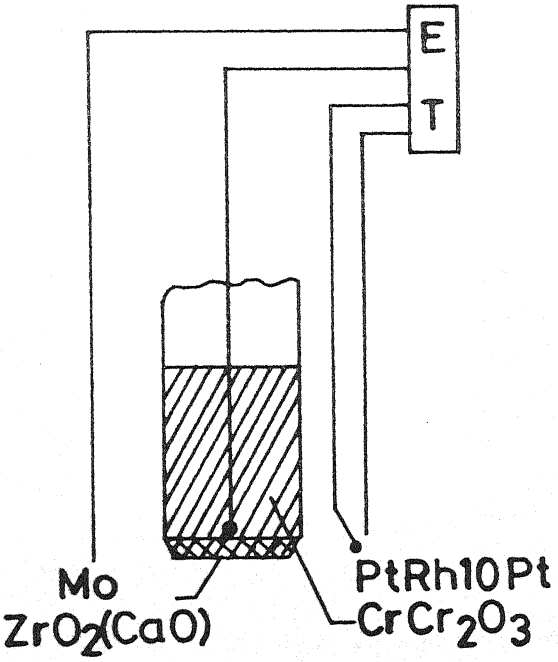

(c) Temp-Q-Tip Sensor

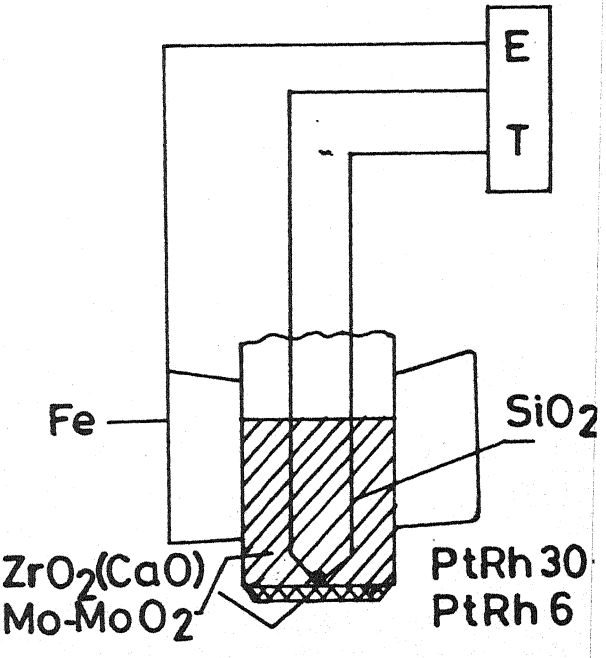

(d) FEA Sensor

ig. 2.1 Schematic Diagram of Commercial Oxygen Sensors.

is a brisk evolution of carbon monoxide, resulting in an outer ingot skin of relatively clean metal low in carbon and other solutes. Such ingots are suited for the manufacture of steel sheets.

Semi-killed steel is deoxidised to a lower extent than killed steel and there is enough oxygen present in the molten steel to react with carbon forming sufficient carbon monoxide to counter-balance the solidification shrinkage. This steel finds application in structural shapes.

Killed steel is deoxidised to such an extent that there is essentially no gas evolution during solidification. Aluminium is generally used for deoxidation together with ferro-alloys of manganese and silicon. In certain cases, calcium silicide or other special strong oxidisers are employed. Killed steel is generally used when a homogeneous structure is required in the finished steel.

2.6 Thermodynamics of Deoxidation of Steel

Deoxidation can be done by addition of a single element like Mn, Si, Al etc. (Fe-M-O type equilibria) or by simultaneous addition of two or more elements. In the former case, the deoxidation products, if solid, has almost unit activity while in the latter case, deoxidation product has lower activity value.

2.6.1 Thermodynamics of Simple Deoxidation

The deoxidation by a single element M can be represented in the following manner

$$aM(l) + \frac{b}{2} O_2(g) = M_aO_b(s,l) \qquad (2.8)$$

change in free energy for reaction (2.17) can be given as

$$\Delta G^\circ = - RT \ln K \qquad (2.9)$$

or,

$$\text{Log } K = - \frac{\Delta G^\circ}{2.303\ RT} \qquad (2.10)$$

The equilibrium constant 'K' is defined as

$$K = \frac{a_{M_aO_b}}{[h_M]^a [h_O]^b} \qquad (2.11)$$

or,

$$\text{Log } K = \text{Log}[a_{M_aO_b}] - \text{Log}[h_M]^a [h_O]^b \qquad (2.12)$$

or,

$$\text{Log}[h_M]^a [h_O]^b = - \text{Log } K + \text{Log}[a_{M_aO_b}] \qquad (2.13)$$

$$\text{Say Log } [h_M]^a [h_O]^b = r \qquad (2.14)$$

$$\therefore \quad r = - \text{Log } K + \text{Log } [a_{M_aO_b}] \qquad (2.15)$$

$a_{M_aO_b}$ represents the activity of M_aO_b (S) with respect to pure solid as standard state and h's are activities with respect to 1 wt percent as standard state.

Now $h_M = f_M[\text{wt \% M}]$ (2.16)

$h_O = f_O[\text{wt\% O}]$ (2.17)

or

$\text{Log}[h_M] = \text{Log}[f_M] + \text{Log}[\text{wt\% M}]$ (2.18)

$\text{Log}[h_O] = \text{Log}[f_O] + \text{Log}[\text{wt\% O}]$ (2.19)

Again,

$\text{Log}[f_M] = e_M^M[\text{wt\% M}] + e_M^O[\text{wt\% O}]$ (2.20)

$\text{Log}[f_O] = e_O^O[\text{wt\% O}] + e_O^M[\text{wt\% M}]$ (2.21)

where f_M is interaction coefficient and e_i^j interaction parameter.

There are some other elements like carbon, sulphur, phosphorus in the bath, which affect the activity coefficients f_M, f_O interms of e_M^C, e_O^C, e_M^S, e_O^S....., so the above equations (2.20) and (2.21) are more precisely written as

$\text{Log}[f_M] = e_M^M[\text{wt\% M}] + e_M^O[\text{wt\% O}] + e_M^i[\text{wt\% i}]$ (2.22)

$\text{Log}[f_O] = e_O^O[\text{wt\% O}] + e_O^M[\text{wt\% M}] + e_O^i[\text{wt\% i}]$ (2.23)

where i = C,S,P.

Considering only the effect of carbon, equations (2.22) and (2.23) can be written as

$\text{Log}[f_M] = e_M^M[\text{wt\% M}] + e_M^O[\text{wt\% O}] + e_M^C[\text{wt\% C}]$ (2.24)

$\text{Log}[f_O] = e_O^O[\text{wt\% O}] + e_O^M[\text{wt\% M}] + e_O^C[\text{wt\% C}]$ (2.25)

Now substituting the value of Log $[f_M]$ and Log $[f_O]$ from equations (2.24) and (2.25) into equations (2.16) to (2.19), we get

$$b \text{ Log}[\text{wt\% }] + (b\, e_O^O + a\, e_M^O)[\text{wt\% O}] = r - a \text{ Log}[\text{wt\% M}]$$

$$-(a\, e_M^M + b\, e_O^M)[\text{wt\% M}] - (a\, e_M^C + b\, e_O^C)[\text{wt\% C}] \qquad (2.26)$$

or,

$$p \text{ Log } x + q\, x = r + S \text{ Log } y + ty + u \text{ carbon} \qquad (2.27)$$

where,

$$p = b$$

$$q = (b\, e_O^O + a\, e_M^O)$$

$$r = -\text{Log } K + \text{Log}[a_{M_a O_b}]$$

$$S = -a$$

$$t = -(a\, e_M^M + b\, e_O^M)$$

$$u = -(a\, e_M^C + b\, e_O^C)$$

and $x = [\text{wt\% O}]$

$y = [\text{wt\% M}]$

Carbon $= [\text{wt\% C}]$. (2.28)

The value of $a_{M_a O_b}$ for simple deoxidation is often taken as one. The equilibrium constant K is given as a function of temperature in the following form

$$\text{Log } K = c/\text{temp} + d \qquad (2.29)$$

The values of c and d for various elements are known from literature[6].

The above principle is applicable only for aluminium and silicon deoxidation and not for manganese deoxidation. In case of manganese, a solid solution (FeO-MnO) type of product is formed and so mole fractions of FeO and MnO have to be considered.

2.6.1.1 Deoxidation with Manganese

Manganese is the weakest deoxidiser of all and so during deoxidation it is followed by addition of other deoxidisers. It is used in form of ferro-manganese. The deoxidation reaction is written as[3]

$$\underline{Mn} + FeO\,(s,l) = MnO\,(s,l) + Fe\,(l) \qquad (2.30)$$

where

$$\text{Log } K_{Mn} = \frac{15050}{\text{temp}} - 6.70 \qquad (2.31)$$

under normal conditions, the composition of reaction product changes continuously with the temperature and the manganese content of the metal. Figure 2.2 gives the manganese-oxygen equilibria[7] at 1600°C.

2.6.1.2 Deoxidation with Silicon

Deoxidation reaction with silicon can be represented as[3]

$$\underline{Si} + \underline{O} = SiO_2 \qquad (2.32)$$

where

$$\text{Log } K_{Si} = \frac{31040}{\text{temp}} - 12.0 \qquad (2.33)$$

When the deoxidiser (e.g. Fe-Si) is plunged into the melt, the oxygen level drops almost instantaneously followed by attainment of a steady value within almost 3-4 minutes after the addition. Figure 2.3 shows the silicon-oxygen equilibria[7] in steel at 1600°C. At 1600°C, 0.004 wt percent silicon in the metal is in equilibrium with 0.088 wt percent oxygen. Hence if the metal contains less than 0.088 wt percent of oxygen, the addition of silicon in excess of 0.004 wt percent produces a solid solution product within the metal. For higher oxygen contents in the metal, the concentration of silica in the deoxidation product is less than the saturation limit and the activity of the silica is less than unity in the reaction product. In practice, a steel which is fully deoxidised or killed contains greater than 0.1 wt percent of residual silicon and so for pure iron-oxygen-silicon melts, the silicon and oxygen in the melt are in equilibrium with silica at approximately unit activity.

2.6.1.3 Deoxidation with Aluminium

Aluminium is widely used as a deoxidiser and is generally regarded as one of the strongest deoxidisers. The deoxidation of steel by aluminium can be written as[3]

$$2\,\underline{Al} + 3\,\underline{O} = Al_2O_3 \qquad (2.34)$$

where,

$$\text{Log } K_{Al} = \frac{62780}{\text{temp}} - 20.54 \qquad (2.35)$$

Deoxidation constant for equation (2.34) can be written as

$$K_{Al} = \frac{a_{Al_2O_3}}{[h_{Al}]^2 [h_o]^3} \qquad (2.36)$$

or,

$$\text{Log } [h_{Al}]^2 [h_o]^3 = - \text{Log } K_{Al} + \text{Log } [a_{Al_2O_3}] \qquad (2.37)$$

Based on thermodynamics of deoxidation of steel, equation (2.26) can be rewritten for aluminium as

$$3 \text{ Log}[\text{wt\% O}] + (3 e_O^O + 2 e_{Al}^O)[\text{wt\% O}] = r - 2 \text{ Log}[\text{wt\% Al}] - (2 e_{Al}^{Al} + 3 e_O^{Al})[\text{wt\% Al}] - (2 e_{Al}^C + 3 e_O^C)[\text{wt\% C}] \qquad (2.38)$$

Equation (2.38) can be represented similar to equation (2.27), i.e.,

$$p \text{ Log } x + q\, y = r + S \text{ Log } y + ty + u \text{ carbon}$$

where

$$p = 3$$

$$q = (3 e_O^O + 2 e_{Al}^O)$$

$$r = - \text{Log } K_{Al} + \text{Log } [a_{Al_2O_3}]$$

$$S = -2$$

$$t = -(2 e_{Al}^{Al} + 3 e_O^{Al})$$

$$u = -(2 e_{Al}^C + 3 e_O^C)$$

$$x = [\text{wt\% O}]$$
$$y = [\text{wt\% Al}] \qquad (2.39)$$

The values of interaction parameters have been taken from the literature[11].

The product of deoxidation with aluminium is either solid alumina or the spinel FeO, Al_2O_3. The spinel is formed only when the aluminium in iron is not in stoichiometric excess of the amount of dissolved oxygen. Generally the deoxidation product is alumina at unit activity. In producing certain extra-deep drawing steels, a low carbon (<0.1% C) steel is killed, usually with a substantial amount of aluminium that is added in the ladle, in the mould or bath. Figure 2.4 gives the aluminium-oxygen equilibria[9] in steel at 1600°C.

Although the deoxidation of steel by aluminium suppresses the formation of carbon monoxide during solidification and hence suppresses blow holes, there are many steel making operations where aluminium killing of steel is undesirable. For example, it is widely recognised that certain alloy steels to be cast as large ingots should not be subjected to aluminium killing because of the piping and deleterious effects of alumina inclusions on the subsequent processing of ingots for certain applications (e.g. generater, rotar shaft).

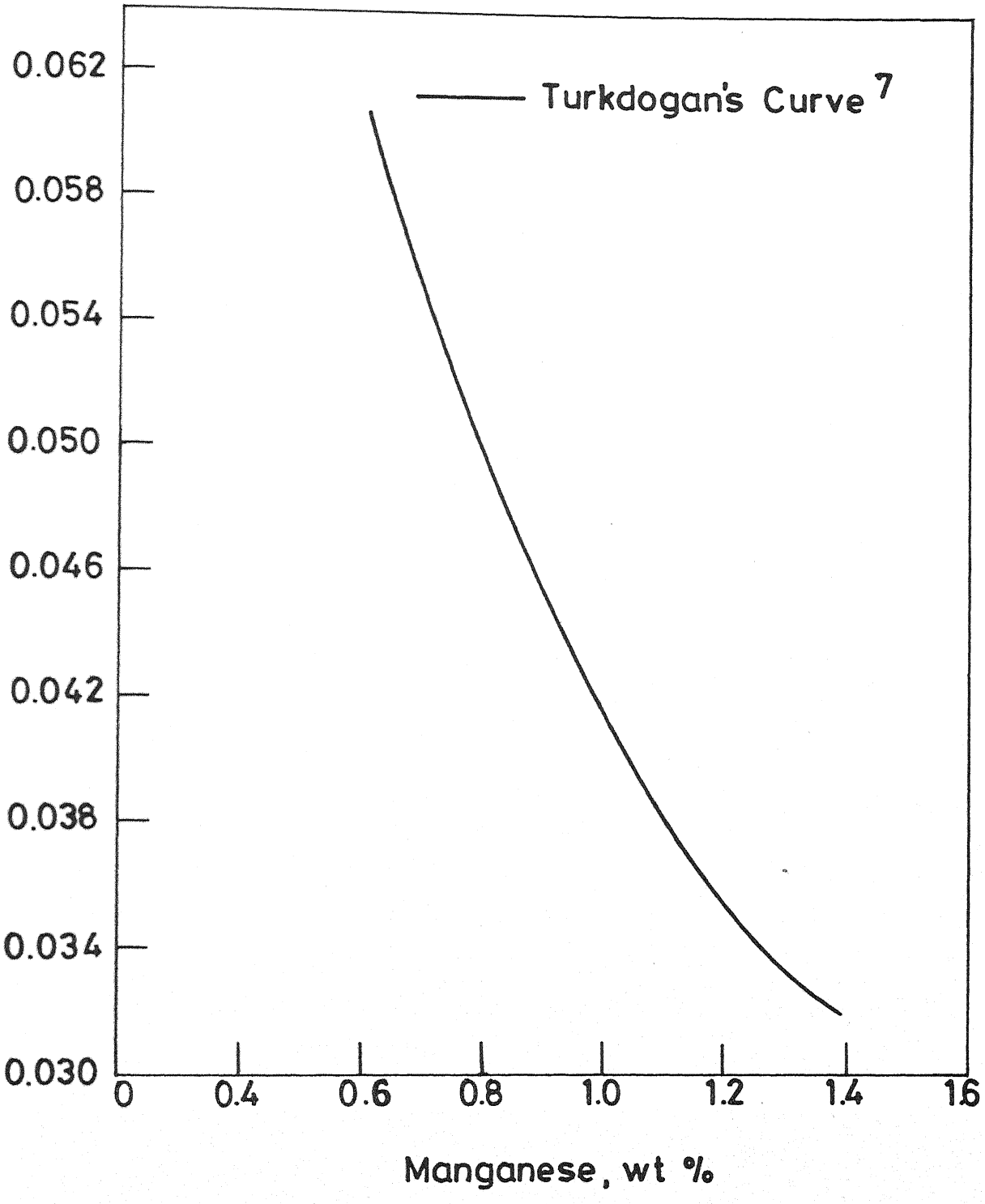

2.2 Comparison of Manganese-Oxygen Equilibria at 1600°C.

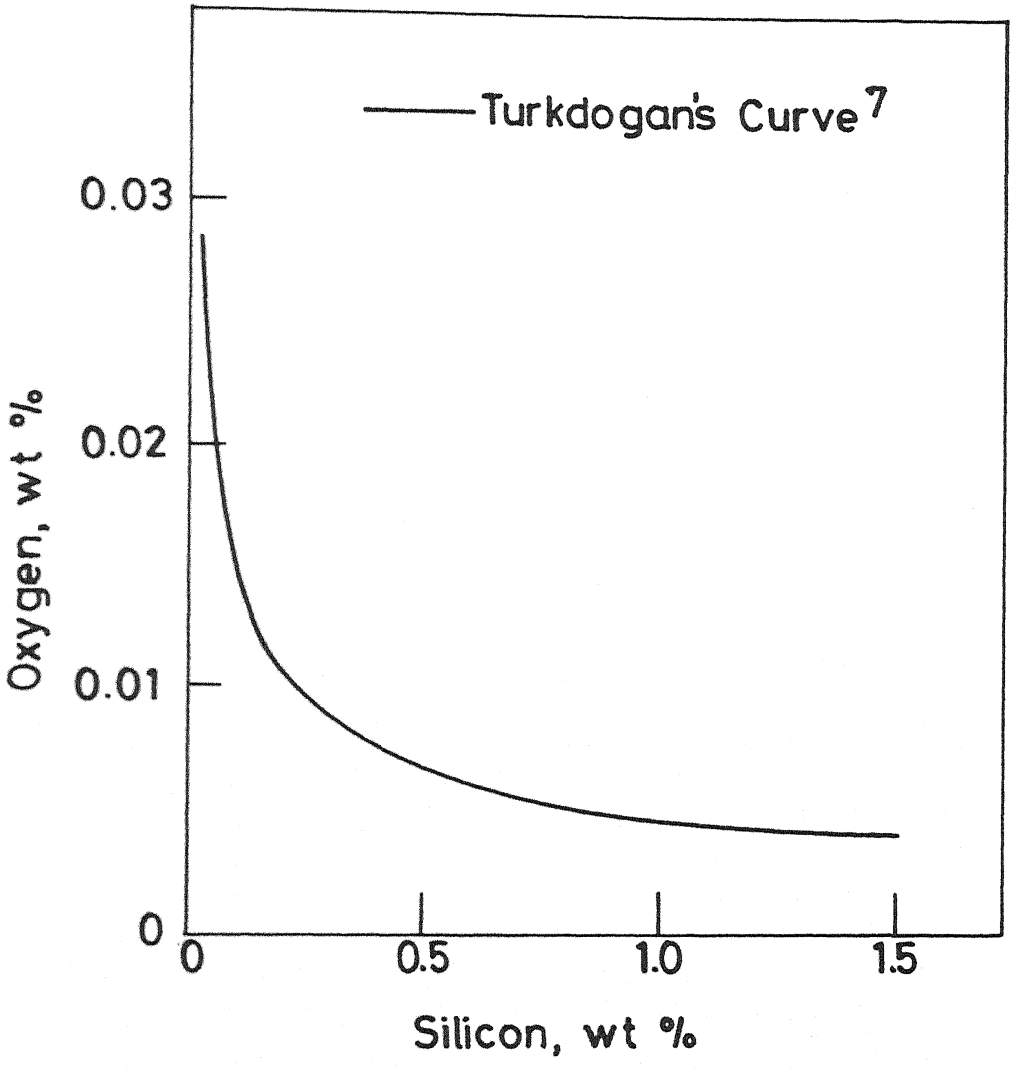

Fig. 2.3 Comparison of Silicon-Oxygen Equilibria in Steel at 1600°C.

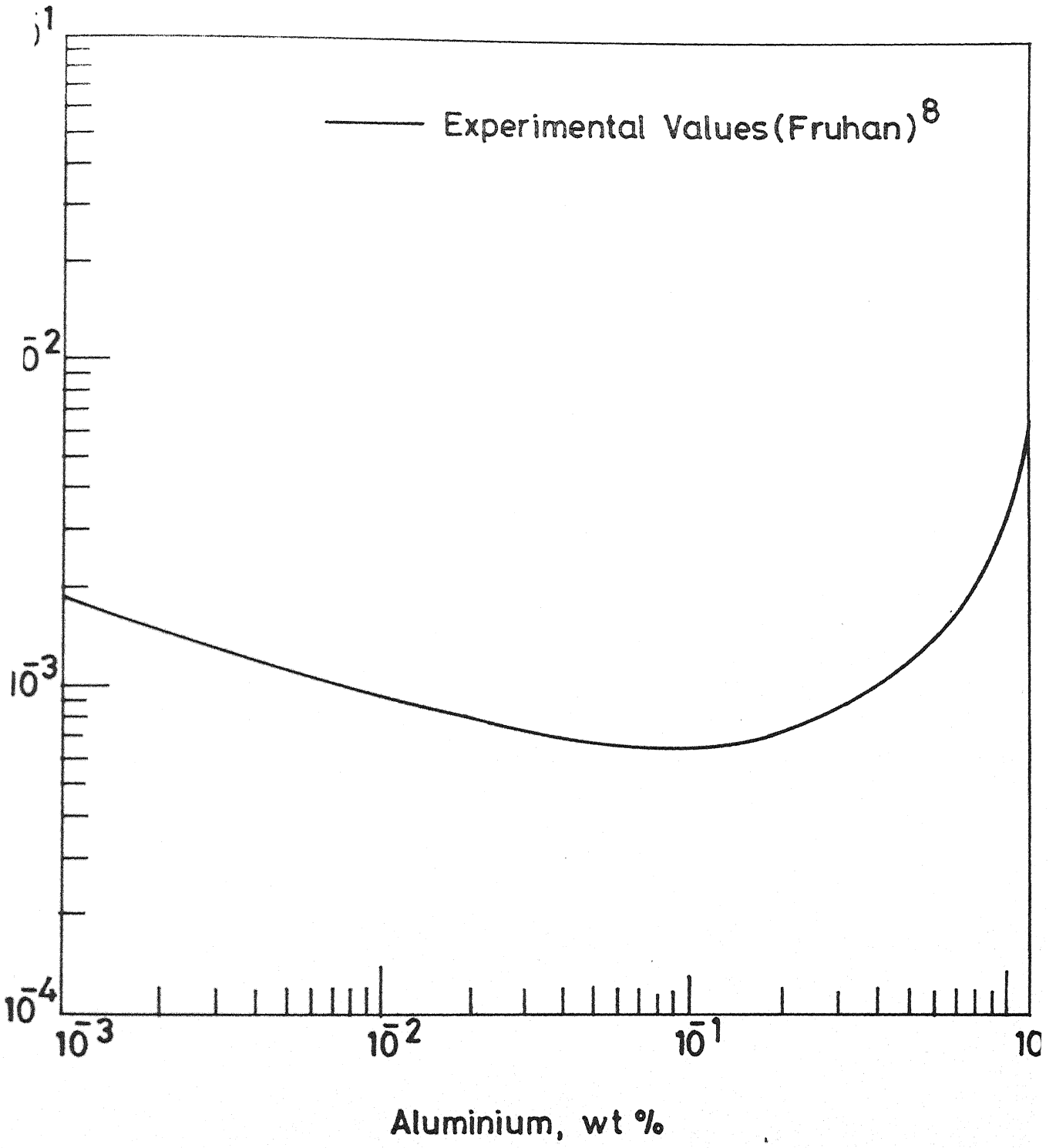

Fig. 2.4 Aluminium-Oxygen Equilibria in Steel at 1600°C.

2.6.2 Thermodynamics of Complex Deoxidation

In comparison to simple deoxidation, the effectiveness of some of the complex deoxidisers has been recognised. Complex deoxidation is nothing but simultaneous addition of two or more deoxidisers viz. silicon-manganese, silicon-calcium, silicon-manganese-aluminium and silicon-calcium-aluminium.

Silicon and manganese are the most widely used deoxidisers added to the steel bath in the furnace and/or in the ladle as ferro-alloys. The extent of deoxidation is more in case of silicon-manganese deoxidation than with silicon alone due to formation of deoxidation product of lower activity value. The deoxidation equilibria[3] is written as

$$\underline{Si} + 2\,MnO = 2\,\underline{Mn} + SiO_2 \qquad (2.40)$$

where the reaction product is a liquid or solid-manganese silicate.

Figure 2.5 shows the activities of residual oxygen and silicon after deoxidation at 1500°C at various activities of residual manganese[7]. Experimental studies have shown that with 0.1 wt percent of silicon in the metal, the deoxidising power of silicon is improved by almost 30 percent when 0.25 wt percent of manganese is added and is almost

doubled by addition of 0.50 percent of manganese .

For equation (2.40), the equilibrium constant is written as

$$K_{Si-Mn} = \frac{(a_{SiO_2})}{(a_{MnO})^2} \cdot \frac{[h_{Mn}]^2}{[h_{Si}]} \qquad (2.41)$$

and

$$\text{Log } K_{Si-Mn} = \frac{8900}{\text{temp}} - 2.948 \qquad (2.42)$$

It is possible to develop an algorithm for finding the equilibrium amounts of silicon, manganese and oxygen in the bath at a given temperature.

The equation (2.41) can be written as

$$\frac{(a_{SiO_2})}{(a_{MnO})^2} = K_{Si-Mn} \cdot \frac{[h_{Si}]}{[h_{Mn}]^2} \qquad (2.43)$$

For different values of $[h_{Si}]$ and $[h_{Mn}]$ and from the knowledge of K_{Si-Mn} from equation (2.42), one can obtain the right hand term of equation (2.43). Here assigning certain values to $[h_{Si}]$ and $[h_{Mn}]$ is equivalent to assuming certain silicon and manganese in the bath. The attempt here is to find corresponding oxygen content at a given temperature.

The activity of silica (a_{SiO_2}) and manganese-oxide (a_{MnO}) and mole fraction of manganese-oxide (N_{MnO}) have been taken from literature[10] as shown in Appendix V. The

relations between (a_{MnO}) vs $(a_{SiO_2})/(a_{MnO})^2$; (a_{SiO_2}) vs $(a_{SiO_2})/(a_{MnO})^2$ and (N_{MnO}) vs $(a_{SiO_2})/(a_{MnO})^2$ are obtained by least square techniques. Now, with the help of equation (2.43), for a particular value of $(a_{SiO_2})/(a_{MnO})^2$, the corresponding values of (a_{SiO_2}), (a_{MnO}) and (N_{MnO}) are calculated. Mole fraction of silica (N_{SiO_2}) can be obtained by the relation:

$$(N_{SiO_2}) = 1.0 - (N_{MnO}) \qquad (2.44)$$

We know that

$$\underline{Mn} + \underline{O} = MnO \qquad (2.45)$$

$$\text{Log } K_{Mn} = 11070/\text{Temp} - 4.526 \qquad (2.46)$$

With the help of equation (2.46), h_o can be obtained because all other parameters are known. With known values of $[h_o, h_{Mn}]$ and $[h_{Si}]$ the values of [wt% O], [wt% Mn] and [wt% Si] can be obtained by the following three simultaneous equations:

$$\text{Log}[h_{Si}] = \text{Log}[\text{wt\% Si}] + e^{Si}_{Si}[\text{wt\% Si}] + e^{Mn}_{Si}[\text{wt\% Mn}] + e^{O}_{Si}[\text{wt\% O}] + e^{C}_{Si}[\text{wt\% C}] \qquad (2.47)$$

$$\text{Log}[h_{Mn}] = \text{Log}[\text{wt\% Mn}] + e^{Mn}_{Mn}[\text{wt\% Mn}] + e^{Si}_{Mn}[\text{wt\% Si}] + e^{O}_{Mn}[\text{wt\% O}] + e^{C}_{Mn}[\text{wt\% C}] \qquad (2.48)$$

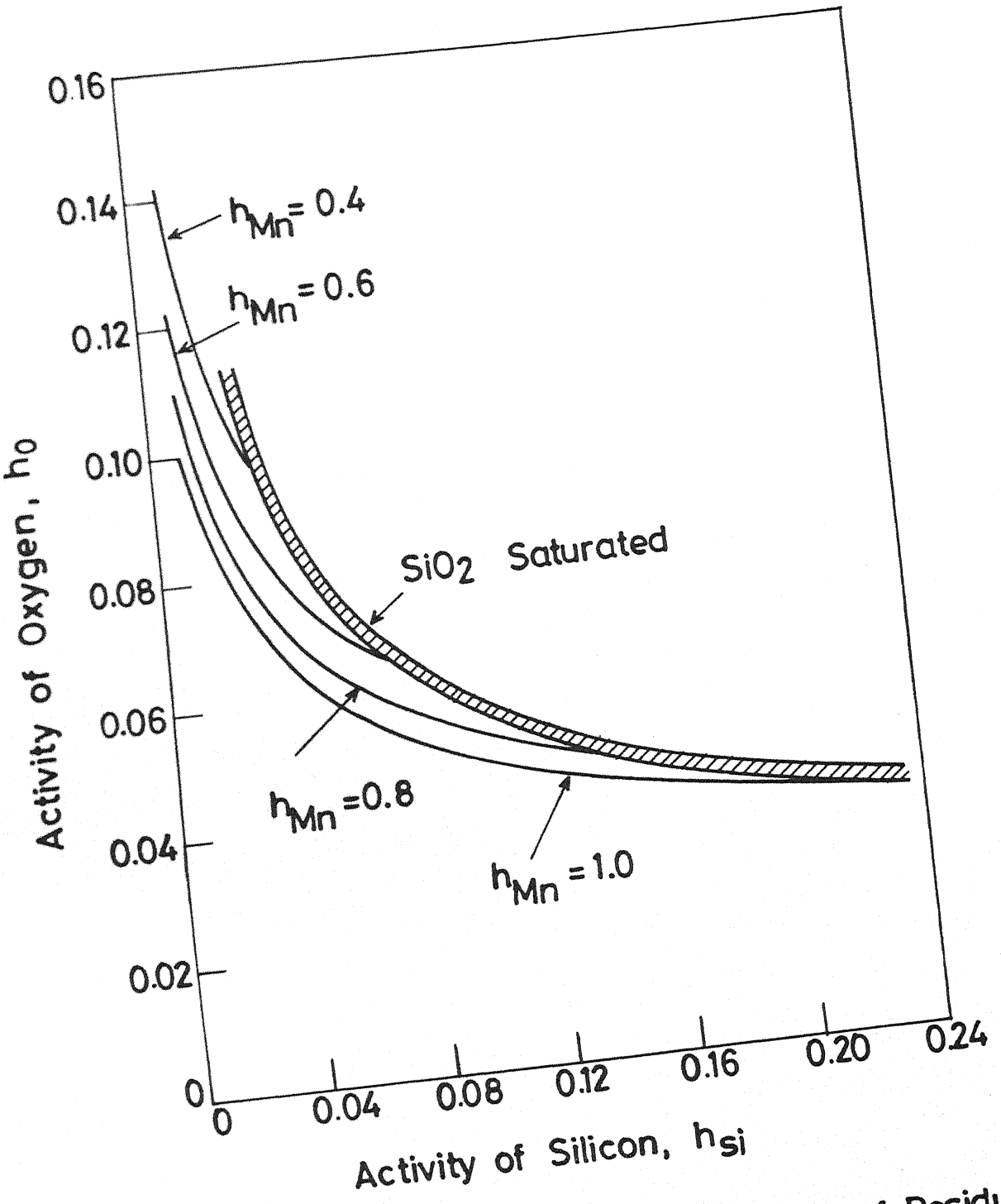

Fig. 2.5 Si+Mn Complex Deoxidation; Activities of Residual Oxygen and Silicon after Deoxidation at 1500°C at Various Activities of Residual Manganese (h_{Mn})

chemical method. In case of any reblows for chemistry and/or temperature adjustments all tests were repeated.

Table 2.1 shows the details of bath analysis at turn down for nineteen experimental heats. Column II shows the recorded temperature for different heat numbers. It is seen that there is a large variation in bath temperature ranging from 1550 to 1735°C. Column III and column IV show the carbon and manganese analysis for different grades of steel respectively. Carbon varies from 0.04 to 0.06 percent, where as manganese from 0.10 to 0.26 percent.

Table 2.2 shows the ladle analysis after deoxidation for different grades of steel for eighteen experimental heats. Column II gives the recorded temperature ranging from 1550 to 1665°C. Manganese varies from 0.28 to 1.15 percent as shown in Column III. As can be seen from the Columns IV and V, variation in the silicon and aluminium concentration is large ranging from 0.02 to 2.0 percent and 0.002 to 0.05 percent respectively.

2.8 Results and Discussion

2.8.1 Activity Measurements at Turndown

Based on nineteen experimental heats at turndown attempt has been made to develop a general regression equation expressing initial bath oxygen content as a function of bath carbon, manganese and turndown temperature. The

general relationship of carbon, manganese and turndown temperature with oxygen activity can be represented as follows:

$$a_o \text{ (ppm)} = X.\text{Temp°C} + Y/\%\ C + Z/\%\ Mn - W \quad (2.50)$$

where a_o = oxygen activity in liquid steel bath (ppm), % C and % Mn denote carbon and manganese contents. X,Y,Z and W are constants.

Now equation (2.50) can be written in the following form

$$Y = \Theta_1 a_1 + \Theta_2 a_2 + \Theta_3 a_3 + \Theta_4 a_4 \quad (2.51)$$

where Y is a dependent variable and a_1, a_2, a_3, a_4 are independent variables. In the present case $a_4 = -1$, Θ_1, Θ_2, Θ_3 and Θ_4 are known as regression coefficients.

Based on the principle of multiple linear regression a computer program was written as shown in Appendix II, which determines the regression coefficients using data from Table 2.1. The coefficients obtained are as follows:

$$\Theta_1 = 0.3885$$
$$\Theta_2 = 10.29$$
$$\Theta_3 = 26.98$$
$$\Theta_4 = -134.09$$

Substituting these values in equation (2.50)

$$a_o(\text{ppm}) = \frac{10.29}{\%\ C} + \frac{26.98}{\%\ Mn} + 0.3885\ \text{Temp°C} + 134.09 \qquad (2.52)$$

This regression equation is valid for steel bath at turndown before deoxidation where carbon ranges from 0.04 to 0.07 percent and manganese is $\leq$ 0.38 percent.

Using the above regression equation, oxygen activities have been back calculated for different experimental values of temperature, percent carbon and percent manganese as shown in Column VI (values range from 492 to 749 ppm). The oxygen activities measured with the oxygen probes also vary largely from 429 to 948 ppm (Column V). One may now compare predicted oxygen values (i.e. from regression equation, Column VI) and the actual values measured with the help of oxygen probes (Column V). The same is shown graphically in Figure 2.6. A program was developed to calculate standard deviation and correlation coefficient based on the principle of linear regression as given in the Appendix I. This gives a standard deviation of $\pm$ 76 ppm and a correlation coefficient 0.291. The low value of correlation coefficient indicates that there is a poor agreement between the oxygen activity values measured with the help of oxygen probes and the oxygen activities obtained with the help of regression equation. A similar type of regression equation was developed for twenty of experimental heats by Banerjee[12] as shown below:

$$a_o(\text{ppm}) = -\frac{2.3548}{\%\ C} + \frac{37.10}{\%\ Mn} + 1.1521\ \text{Temp}^\circ C - 1487.82 \quad (2.53)$$

The standard deviation reported for equation (2.53) is $\pm$ 130 ppm which is larger than for equation (2.52). In any case both the regression equations (2.52) and (2.53) are associated with a large standard deviation and poor correlation coefficient (less than 0.3) and therefore are not acceptable. It demonstrates that under industrial conditions oxygen activity in the bath is very poorly related to carbon, manganese and temperature of bath, i.e. the bath is far from equilibrium at turndown and no equations can be used to predict oxygen activity based on bath composition and temperature. Further, equation (2.53) reported by Banerjee[12] has a negative coefficient for carbon. This is not correct as from thermodynamics the expected relationship of carbon and oxygen is of the form $a_o(\text{ppm}) \propto \frac{1}{\%\ C}$.

2.8.2 Activity Measurements after Deoxidation

Oxygen activities in the ladle after deoxidation ranged from 7 to 87 ppm in the eighteen experimental heats as shown in Column VI of Table 2.2. Attempt was made to find out the thermodynamic equilibrium oxygen concentration for simple aluminium deoxidation and for complex silicon-manganese deoxidation and then compare these with the oxygen activity values measured with

oxygen probes. As discussed earlier in section 2.6.1.3 and 2.6.2, the simple aluminium and complex silicon-manganese deoxidation reactions are represented as

$$2\,\underline{Al} + 3\,\underline{O} = Al_2O_3$$

$$\underline{Si} + 2\,MnO = SiO_2 + 2\,Mn$$

Principles for finding the equilibrium oxygen concentration based on the above reactions have been discussed in sections 2.6.1.3 and 2.6.2 and the computer programs are given in Appendix III and Appendix IV. The oxygen concentrationscalculated considering simple aluminium deoxidation and complex silicon-manganese deoxidation are given in the Columns VII and VIII respectively. It can be seen that there are large differences between oxygen probe values and thermodynamically calculated oxygen values in the case of silicon-manganese deoxidation ranging from 85 to 576 ppm. The same is shown graphically in Figure 2.7. In case of aluminium deoxidation also, agreement is poor. This is evident from the Figure 2.8, where again oxygen probe values have been plotted against theoretically calculated values.

If calculations are made for complex deoxidiser like silicon-manganese-aluminium, the theoretically calculated oxygen values will be still lower than simple aluminium or silicon-manganese deoxidation.

TABLE 2.1 : Details of Oxygen Activities and Bath Analysis at Turndown (Data obtained from trials at Rourkela Steel Plant, Rourkela)

Sl. No.	Temp(°C)	% C	% Mn	Probe oxygen (ppm)	Predicted oxygen (ppm)
1.	1599	0.04	0.10	672	723.26
2.	1610	0.04	0.10	485	723.69
3.	1625	0.04	0.10	475	724.27
4.	1650	0.06	0.22	664	492.33
5.	1640	0.04	0.10	705	724.85
6.	1620	0.04	0.10	793	724.07
7.	1660	0.04	0.10	948	725.63
8.	1660	0.05	0.11	825	749.65
9.	1735	0.04	0.14	779	651.46
10.	1650	0.04	0.14	503	648.16
11.	1640	0.04	0.12	809	679.89
12.	1685	0.04	0.12	707	681.64
13.	1626	0.04	0.12	724	538.32
14.	1650	0.06	0.16	469	509.48
15.	1694	0.05	0.26	429	648.55
16.	1660	0.04	0.14	583	624.94
17.	1550	0.05	0.12	575	648.48
18.	1630	0.05	0.11	651	596.86
19.	1654	0.05	0.14	556	619.34

TABLE 2.2 : Details of Oxygen Activities and Ladle Analysis after Deoxidation (Data obtained from trials at Rourkela Steel Plant, Rourkela)

Sl. No.	Temp (°C)	% Mn	% Si	% Al	Probe oxygen (ppm)	Theoretical oxygen (Al)	Theoretical oxygen (Si + Mn)
1.	1565	0.40	1.54	0.020	76	4	115
2.	1580	0.40	1.50	0.002	25	23	130
3.	1550	0.38	1.50	0.002	11	15	101
4.	1620	0.40	0.02	0.03	8	8	407
5.	1590	0.45	1.76	0.05	17	4	141
6.	1640	0.62	1.58	0.004	17	34	192
7.	1665	0.40	0.02	0.044	87	12	576
8.	1560	0.28	1.65	0.002	17	17	127
9.	1575	0.38	2.0	0.005	7	12	137
10.	1560	0.80	1.02	0.008	21	7	85
11.	1570	0.62	1.03	0.036	27	4	101
12.	1590	1.15	0.24	0.012	28	8	121
13.	1565	0.54	1.02	0.004	11	12	100
14.	1610	0.36	0.02	0.012	36	11	373
15.	1600	0.71	0.175	0.028	11	6	163
16.	1620	0.72	0.181	0.020	34	10	193
17.	1650	0.72	0.165	0.008	78	25	253
18.	1600	0.34	0.02	0.05	30	5	347

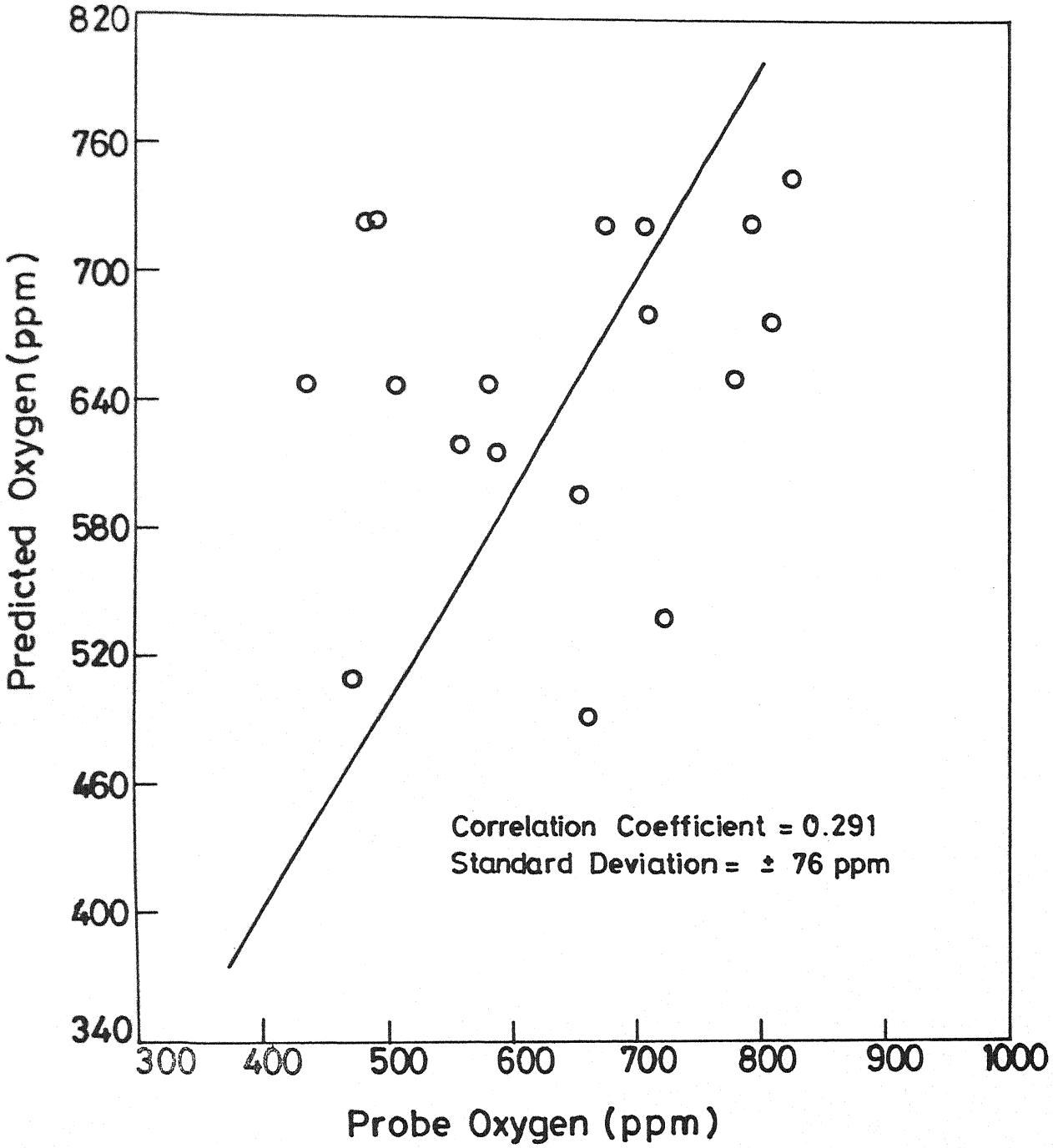

Fig. 2.6 Plot of Oxygen Activity Measured by CELOX Probes at Turndown and Predicted Oxygen from Regression Equation —
a_o (ppm) = 10.29 / % C + 26.98 / % Mn + 0.3885 Temperature (°C) + 134.09.

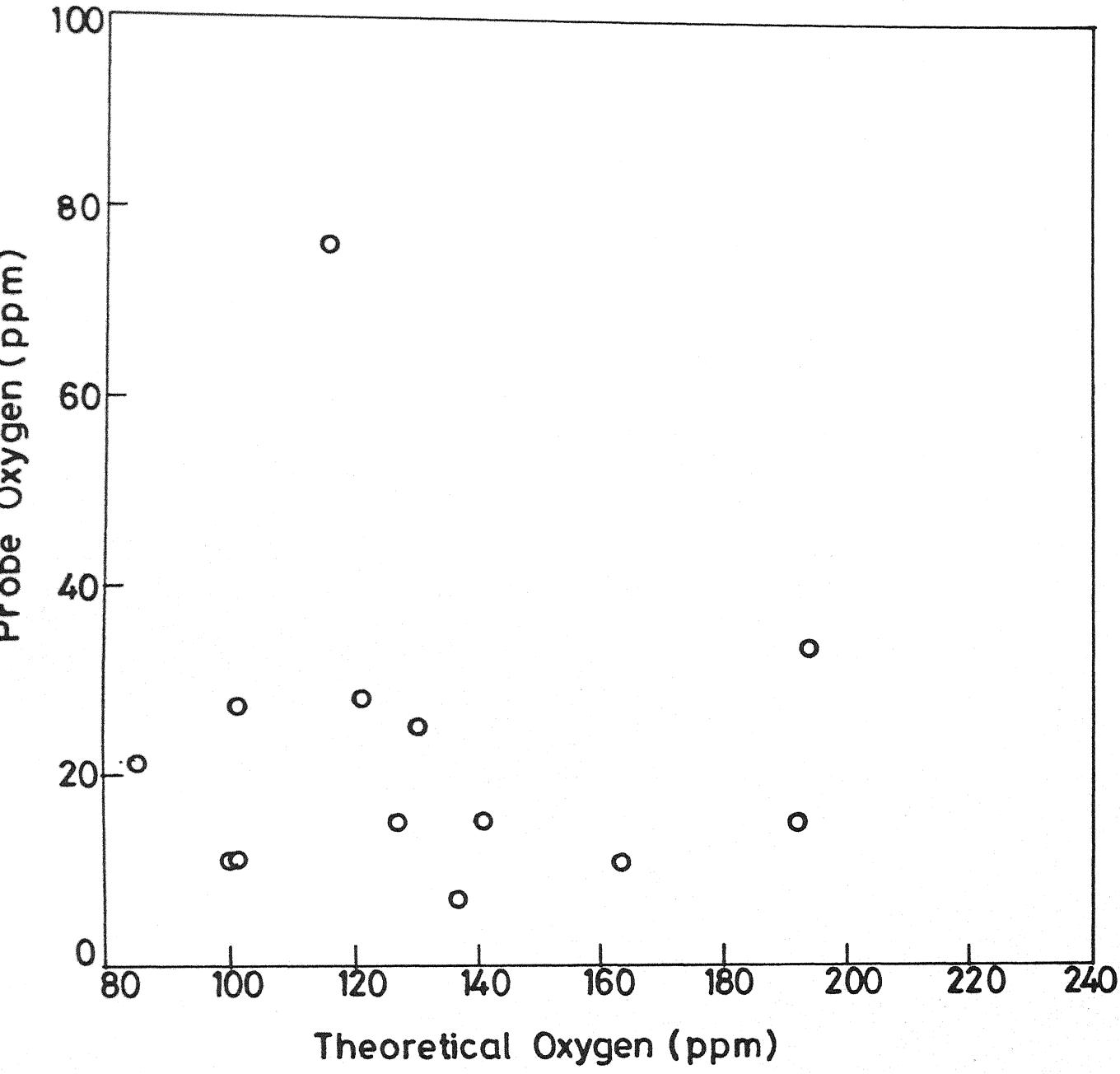

Fig. 2.7 Relation Between Oxygen Activity Measured by CELOX Probes and Oxygen Activity Determined from Thermodynamics of Deoxidation Reaction ($\underline{Si} + 2MnO = SiO_2 + 2Mn$)

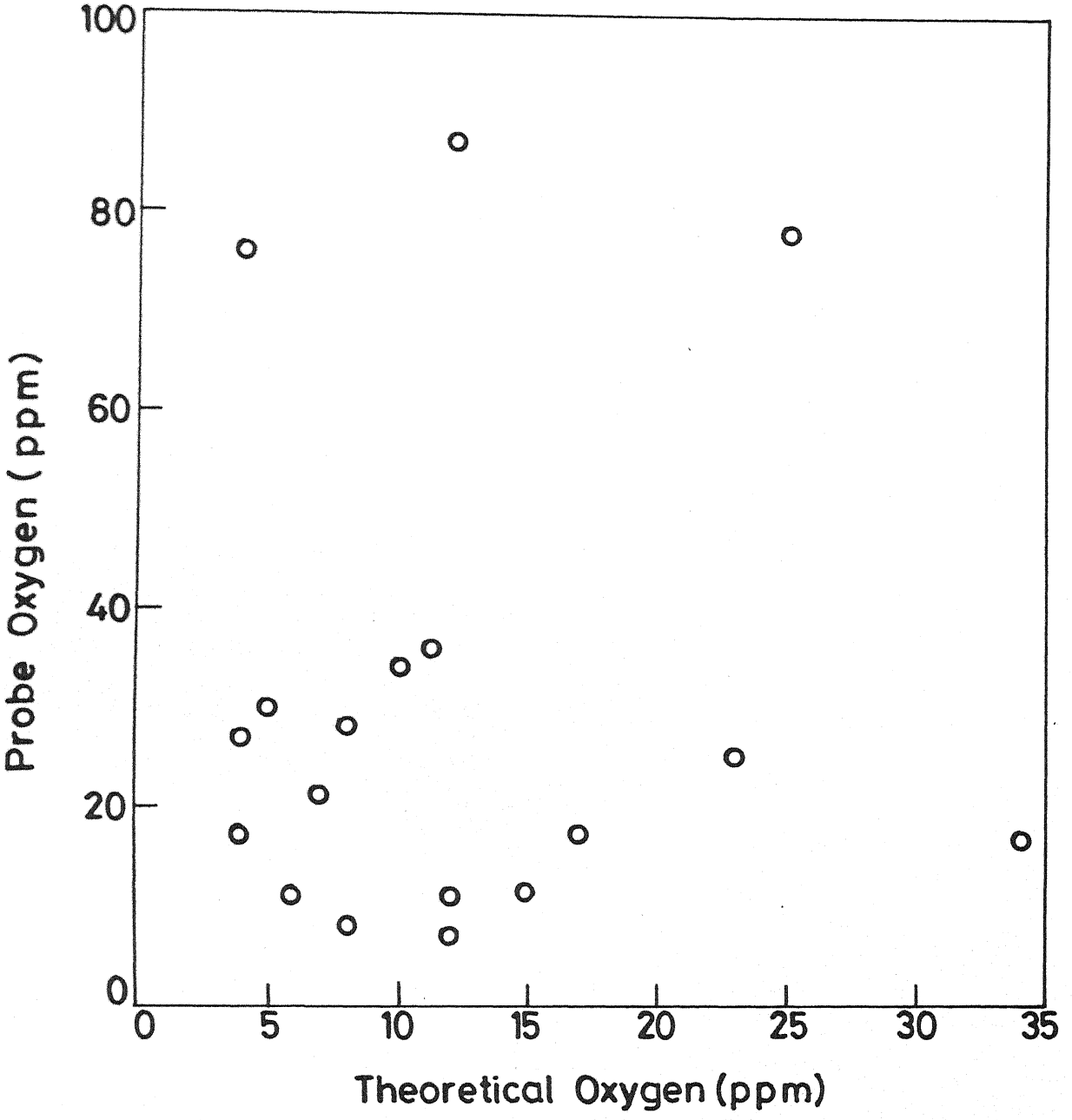

Fig.2.8 Relation Between Oxygen Activity Measured by CELOX probes and Oxygen Activity Determined from Thermodynamics of Deoxidation Reaction ($2\underline{Al} + 3\underline{O} = Al_2O_3$)

From the above discussion, it is evident that equilibrium is not attained in the ladle and measured oxygen activity is very poorly related to bath composition. The use of oxygen probes to monitor deoxidation practices under the conditions existing in the oxygen steel making shops appears difficult to put into practice. Oxygen probes may be used only as an approximate guide in making deoxidation additions. However, if more time is allowed for the equilibrium to be attained or if metal is stirred in any one of the ladle metallurgical operations then measured oxygen values will be closer to equilibrium or thermodynamically calculated values (based on bath composition)

Under these conditions oxygen probes readings may be used to control the amount of oxygen dissolved in liquid steel in subsequent steps, i.e. just after ladle metallurgical treatment and before casting.

2.9 Conclusions

(1) Based on industrial data, a regression equation was established between oxygen activity measured at turndown and bath composition and temperature as

$$a_o(\text{ppm}) = \frac{10.29}{\%\ C} + \frac{26.98}{\%\ Mn} + 0.3885\ \text{Temp}^\circ C + 134.09.$$

The correlation coefficient for this equation is very poor (.3) suggesting that bath is far from equilibrium at turndown.

(2) A comparison of oxygen activities measured with oxygen probes and thermodynamically calculated oxygen activities after deoxidation in the ladle again show that the bath did not attain equilibrium. Measured values were higher than corresponding predicted values in equilibrium with aluminium content of bath. The opposite was true for complex silicon-manganese deoxidation calculations based on silicon and manganese content of bath. There is no need to do Al-Si-Mn deoxidation calculations as this would predict oxygen activity values lower than that simple aluminium deoxidation.

(3) Oxygen sensor may be used only as an approximate tool in controlling deoxidation practice unless a longer time is allowed for equilibration viz. in the ladle metallurgical treatments where argon purging is used to homogenise the bath and allow more time for deoxidation products to float up.

REFERENCES

1. Elliott, J.F., Gleiser, M. and Ramakrishna, V., Thermochemistry for Steelmaking; Vol.2, Addition, Wesley, Reading Mass, U.S.A. (1963)

2. Floridis, T.P. and Chipman, J., Trans. Amer. Inst. Mining, Met. Petrol Engrs, 212, 549 (1958).

3. Bodsworth, C., Physical Chemistry of Iron and Steel Manufacture.

4. Suzuki, K., Ejima, A., Kato, M. and Sanbongi, K., Transactions ISU, Vol. 17, 1977, p-477.

5. Richards, S.R., BHP Tech., Bulletin 18,2 (1974),p-24.

6. Olette, M. and Gatellier, C., Deoxidation of Liquid Steel, Information Symposium: Casting and Solidification of Steel, Luxembourg, 29 Nov. to 1 Dec., 1977, Vol.1, p-34.

7. Turkdogan, E.T., Deoxidation of Steel, Proceedings of International Conference on Metallurgical Chemistry held at U. of Sheffield, England, July 1971.

8. Fruhan, R.J., Trans. Met. Soc., AIME, Vol. 245, p-1215.

9. Turkdogan, E.T., J. of Iron and Steel Inst., Jan. 1972, p-21.

10. Abraham, K.P., Davis, M.W. and Richardson, F.D., TISI, 1960, Vol. 196, p-82.

11. Sigworth, G.K. and Elliott, J.F., Metal Science, 1974, Vol. B, page-298.

12. Banerjee, U.K., RDCIS-SAIL, Rourkela Steel Plant, Rourkela, Private communications.

SUGGESTIONS FOR FURTHER WORK

1. Experiments of Banya and Matoba may be done for high carbon alloys to find out the dependence of interaction parameter e_C^O/e_O^C on carbon content.
2. In the above experiments oxygen probes may be used for direct determination of oxygen activity rather than employing an analytical method to determine oxygen dissolved in steel.

APPENDIX-I

```
C
C LEAST SQUARE TECHNIQUE
      DIMENSION X(19),Y(19)
      OPEN(UNIT=6,DEVICE='DSK',FILE='LIN.DAT')
      READ(6,*)(X(I),Y(I),I=1,19)
      SX=0
      SY=0
      SX2=0
      SY2=0
      SXY=0
      DO 20 I=1,19
      X1=X(I)
      Y1=Y(I)
      SX=SX+X1
      SY=SY+Y1
      SX2=SX2+X1*X1
      SY2=SY2+Y1*Y1
      SXY=SXY+X1*Y1
   20 CONTINUE
      B=(19.*SXY-SX*SY)/(19.*SX2-SX*SX)
      A=(SY-B*SX)/19.
      S2YX=(SY2-A*SY-B*SXY)/(19.-2.)
      R=(19.*SXY-SX*SY)/(SQRT(19.*SX2-SX*SX)*SQRT(19.*SY2-SY*SY))
      STDDEV=SQRT(S2YX)
      WRITE(55,*)A,B,R,STDDEV
      STOP
      END
```

```
C       THIS NAG SUBROUTINE(G02CJF) CALCULATES REGRESSION COEFFICIENTS
C       AND STANDARD ERROR OF ESTIMATION FOR COEFFICIENTS
        REAL X(23,3),Y(23,1),THETA(3,1),SIGSQ(1),C(23,3),WK1(3,4),
       1 WK2(23)
        REAL VT1,VT2,VT3
        INTEGER IPIV(3)
        N=23;M=3;IR=1;IX=N;IT=M;IC=N;IFAIL=0;IY=N
        READ(22,*)(Y(I,IR),I=1,N)
        READ(22,*)(X(I,1),I=1,N)
        READ(22,*)(X(I,2),I=1,N)
        DO 100 I=1,23
        X(I,3)=1.
100     CONTINUE
        CALL G02CJF(X,IX,Y,IY,N,M,IR,THETA,IT,SIGSQ,C,IC,IPIV,WK1,WK2,
       1 IFAIL)
        VT1=SIGSQ(1)*C(1,1)
        VT2=SIGSQ(1)*C(2,2)
        VT3=SIGSQ(1)*C(3,3)
        SEE1=SQRT(VT1)
        SEE2=SQRT(VT2)
        SEE3=SQRT(VT3)
        SEE4=SQRT(SIGSQ(1))
        WRITE(23,*)IFAIL
        WRITE(23,*)THETA(1,1),THETA(2,1),THETA(3,1),SEE1,SEE2,SEE3,SEE4
        STOP
        END
```

```
C       SIMPLE ALUMINIUM DEOXIDATION
        DIMENSION AX(27),AY(27),TEMP(27)
        OPEN (UNIT=21,DEVICE='DSK',FILE='AL.DAT')
        OPEN (UNIT=1,DEVICE='DSK',FILE='FL.DAT')
        CARBON=0.0
        DO 20 III=1,18
        X=0.0002
        READ(21,*)TEMP(III) , AY(III)
        TEMP(III)=TEMP(III)+273.0
        WRITE(1,31)TEMP(III),CARBON
31      FORMAT(/,20X,'TEMP =',F7.1,' DEG KEL',//,20X,'CARBON =',F5.2,/
        EALAL=63./TEMP(III)+0.011;EOAL=-34740./TEMP(III)+11.95
        EOO=-1750./TEMP(III)+0.734
        EALO=-20600./TEMP(III)+7.15
        ECAL=.091;ECO=-.45
        DATA A,B,C,D /2.,3.,62780.,-20.54/
        AAL2O3=1.
        ALOGK=C/TEMP(III)+D
        P=B
        Q=B*EOO+A*EOAL
        R=-ALOGK+ALOG10 (AAL2O3)
        T=-(A*EALAL+B*EALO)
        S=-A
        U=-(A*ECAL+B*ECO)
        Y=AY(III)
99      CALL SOLU(P,Q,R,S,T,U,CARBON,Y,X)
        AX(III)=X
11      WRITE(1,5) AY(III),AX(III)
5       FORMAT(10X,'ALUM %=',E10.3,3X,'OXYGEN %=',E10.3)
20      CONTINUE
        STOP;END
```

```
      SUBROUTINE SOLU (P,Q,R,S,T,U,CARBON,Y,X)
      I=0;CC=R+S*ALOG10(Y)+T*Y+U*CARBON;XN=0
1     F1=P*ALOG10(X)+Q*X-CC
      F2=P/2.303/X+Q
      I=I+1;XN=X-F1/F2;E=XN/1000000.
      IF (ABS(XN-X)<ABS(E)) GO TO 2
      X=XN
      IF (I.LT.500) GO TO 1
5     FORMAT( 'NO CONVERG FOR X='E10.3,' Y='E10.3)
      RETURN
2     X=XN
      RETURN;END
```

```
SILICON-MANGANESE DEOXIDATION
IMPLICIT REAL (A-H,J-Z)
INTEGER I,N,L
DIMENSION RX(20),RY(20),RZ(20),RW(20),XX(20),YY(20),WW(20),ZZ(20)
DIMENSION A(3),C(3),B(3,3)
N=4
MWO=16; MWMN=55;MWSI=28
ESISI=0.32; EMNSI=0.060;EOSI=-0.14;ECMN=-0.012
ESIMN=0.033;EMNMN=-0.003;EOMN=-0.03;ECSI=0.08;ECO=-0.33
ESIO=-0.25;EMNO=-0.083;EOO=0.0
B(1,1)=ESISI;B(1,2)=EMNSI;B(1,3)=EOSI
B(2,1)=ESIMN;B(2,2)=EMNMN;B(2,3)=EOMN
B(3,1)=ESIO ;B(3,2)=EMNO ;B(3,3)=EOO
READ(22,*)(RY(I),RW(I),RZ(I),I=1,N)
WRITE(1,12)(RY(I),RW(I),RZ(I),I=1,N)
FORMAT(10X,'AMNO=',F6.3,'     AMNO=',F6.3,'     ASIO2=',F6.3)
DO  11 I=1,N
RX(I)=RZ(I)/RW(I)/RW(I)
YY(I)=ALOG10(RY(I))
ZZ(I)=ALOG10(RZ(I))
WW(I)=ALOG10(RW(I))
XX(I)=ALOG10(RX(I))
CALL COEFF(XX,WW,N,ASLOPE,ACONST)
CALL COEFF(XX,YY,N,SLOPE,CONST)
CALL COEFF(XX,ZZ,N,BSLOPE,BCONST)
WRITE(1,18)ASLOPE,ACONST,BSLOPE,BCONST,SLOPE,CONST
FORMAT(//,10X,'ASLOPE=',E10.3,'   ACONST=',E10.3,'   BSLOPE=',
1  E10.3,'   BCONST=',E10.3,'   SLOPE=',E10.3,'   CONST=',E10.3
2 ,//)
DO 3 K=1,18
READ(31,*)CARBON,TEMP,WSI1,WMN1
```

```
WO=0.0
DO 37 IJ=1,1
K8=10**(8900.0/TEMP-2.948)
FSI=10.0**(ESISI*WSI1+ESIMN*WMN1+ESIC*CARBON+ESIO*WO)
FMN=10.0**(EMNMN*WMN1+EMNSI*WSI1+EMNC*CARBON+EMNO*WO)
FO=10.0**(EOO*WO+EOMN*WMN1+EOSI*WSI1+EOC*CARBON)
HMN=WMN1*FMN
HSI=WSI1*FSI
XP=K8*HSI/HMN/HMN
AMNO=XP**ASLOPE*10**ACONST
ASIO2=XP**BSLOPE*10**BCONST
NMNO=XP**SLORE*10**CONST
NSIO2=1.0-NMNO
IF(ASIO2.GT.1.0) GO TO 3
IF(AMNO.GT.1.0) GO TO 3
K7=10**(11070.0/TEMP-4.526)
HO=AMNO/HMN/K7
A(1)=ALOG10(HSI); C(1)=HSI
A(2)=ALOG10(HMN); C(2)=HMN
A(3)=ALOG10(HO) ; C(3)=HO
A(1)=A(1)- ECSI*CARBON
A(2)=A(2)- ECMN*CARBON
A(3)=A(3)- ECO*CARBON
CALL WEIGHT(A,B,C)
WO=C(3)
CONTINUE
WRITE(1,33)CARBON,TEMP,WMN1,WSI1,WO
FORMAT(4X,'CARBON = ',F6.3,'  TEMPERATURE = ',
1 F7.2,'  MANGANESE = ',F6.3,' SILICON = ',F7.4,
2 '  OXYGEN = ',F7.4)
CONTINUE
STOP; END
SUBROUTINE COEFF(AX,Y,N,SLOPE,CONST)
DIMENSION AX(20),Y(20)
SX=0.0;SXX=0.0;SYY=0.0;SY=0.0;SXY=0.0
```

```
DO 10 I=1,N
SX=SX+AX(I)!FINDING THE SUM OF X
SXX=SXX+AX(I)*AX(I)
SYY=SYY+Y(I)*Y(I)
SY=SY+Y(I)
SXY=SXY+AX(I)*Y(I)
SLOPE=(SXY-SX*SY/N)/(SXX-SX*SX/N)
CONST=(SX*SXY-SY*SXX)/(SX *SX-N*SXX)
SGX=SQRT(SXX/N-SX*SX/N/N)
SGY=SQRT(SYY/N-SY*SY/N/N)
XB=SX/N;YB=SY/N
R=(SXY-N*XB*YB)/N/SGX/SGY
WRITE(5,88)R,SX,SY,SXX,SYY,SXY,SGX,SGY,XB,YB,SLOPE,CONST

FORMAT('      R='12E12.6)
RETURN;END
SUBROUTINE WEIGHT(H,B,X)
DIMENSION B(3,3),H(3),X(3),D(3,3),G(3),XX(3)
L=3
IC=0
DO 10 I=1,L
G(I)=ALOG10(X(I))-H(I)
DO 10 J=1,L
G(I)=G(I)+B(I,J)*X(J)
DO 11 I=1,L
DO 12 J=1,L
D(I,J)=B(I,J)
D(I,I)=D(I,I)+1.0/X(I)/2.303
CALL SOLVE(D,G)
YMAX=0.0
DO 15 I=1,L
X(I)=X(I)-G(I)
IF (ABS(G(I)/X(I)).GT.YMAX)YMAX=ABS(G(I)/X(I))
CONTINUE
ERROR =1.E-7
```

```
IF(I*AY<ERROR)RETURN
IC=IC+1
IF(IC<100) GO TO 1
RETURN;END

SUBROUTINE SOLVE(A,G)
READ A(3,3),G(3)
L=3
DO 10 I=1,L-1
DO 10 J=I+1,L
R=A(J,I)/A(I,I)
G(J)=G(J)-G(I)*R
DO 10 K=1,L
A(J,K)=A(J,K)-A(I,K)*R
DO 11 I=L,2,-1
DO 11 J=I-1,1,-1
R=A(J,I)/A(I,I)
G(J)=G(J)-G(I)*R
DO 11 K=I,L
A(J,K)=A(J,K)-A(I,K)*R
DO 12 I=1,L
G(I)=G(I)/A(I,I)
RETURN;END
```

TEMP = 1838.0 DEG KEL
CARBON = 0.00
ALUM %= 0.200E-01 OXYGEN %= 0.475E-03
TEMP = 1853.0 DEG KEL
CARBON = 0.00
ALUM %= 0.200E-02 OXYGEN %= 0.235E-02
TEMP = 1823.0 DEG KEL
CARBON = 0.00
ALUM %= 0.200E-02 OXYGEN %= 0.152E-02
TEMP = 1893.0 DEG KEL
CARBON = 0.00
ALUM %= 0.300E-01 OXYGEN %= 0.836E-03
TEMP = 1863.0 DEG KEL
CARBON = 0.00
ALUM %= 0.500E-01 OXYGEN %= 0.476E-03
TEMP = 1913.0 DEG KEL
CARBON = 0.00
ALUM %= 0.400E-02 OXYGEN %= 0.343E-02
TEMP = 1938.0 DEG KEL
CARBON = 0.00
ALUM %= 0.440E-01 OXYGEN %= 0.129E-02
TEMP = 1833.0 DEG KEL
CARBON = 0.00
ALUM %= 0.200E-02 OXYGEN %= 0.176E-02
TEMP = 1848.0 DEG KEL
CARBON = 0.00
ALUM %= 0.500E-02 OXYGEN %= 0.121E-02
TEMP = 1833.0 DEG KEL
CARBON = 0.00
ALUM %= 0.800E-02 OXYGEN %= 0.731E-03
TEMP = 1843.0 DEG KEL
CARBON = 0.00

ALUM %= 0.360E-01 OXYGEN %= 0.398E-03
TEMP = 1863.0 DEG KEL
CARBON = 0.00
ALUM %= 0.120E-01 OXYGEN %= 0.881E-03
TEMP = 1838.0 DEG KEL
CARBON = 0.00
ALUM %= 0.400E-02 OXYGEN %= 0.121E-02
TEMP = 1883.0 DEG KEL
CARBON = 0.00
ALUM %= 0.120E-01 OXYGEN %= 0.116E-02
TEMP = 1873.0 DEG KEL
CARBON = 0.00
ALUM %= 0.280E-01 OXYGEN %= 0.659E-03
TEMP = 1893.0 DEG KEL
CARBON = 0.00
ALUM %= 0.200E-01 OXYGEN %= 0.101E-02
TEMP = 1923.0 DEG KEL
CARBON = 0.00
ALUM %= 0.800E-02 OXYGEN %= 0.252E-02
TEMP = 1873.0 DEG KEL
CARBON = 0.00
ALUM %= 0.500E-01 OXYGEN %= 0.543E-03